

Illinois State University

ISU ReD: Research and eData

---

Theses and Dissertations

---

2017

## Formation, Characterization, and Optimization of Antibody-Gold Nanoparticle Conjugates

Seth L. Filbrun

Illinois State University, [sfilbr@ilstu.edu](mailto:sfilbr@ilstu.edu)

Follow this and additional works at: <https://ir.library.illinoisstate.edu/etd>

 Part of the [Chemistry Commons](#)

---

### Recommended Citation

Filbrun, Seth L., "Formation, Characterization, and Optimization of Antibody-Gold Nanoparticle Conjugates" (2017). *Theses and Dissertations*. 668.

<https://ir.library.illinoisstate.edu/etd/668>

This Thesis-Open Access is brought to you for free and open access by ISU ReD: Research and eData. It has been accepted for inclusion in Theses and Dissertations by an authorized administrator of ISU ReD: Research and eData. For more information, please contact [ISUREd@ilstu.edu](mailto:ISUREd@ilstu.edu).

# FORMATION, CHARACTERIZATION, AND OPTIMIZATION OF ANTIBODY-GOLD NANOPARTICLE CONJUGATES

Seth L. Filbrun

75 Pages

Protein modified gold nanoparticle based immunoassays are the basis of many novel detection techniques. There are many groups working on novel immunoassays but there is still much to understand about how many proteins are attached onto each nanoparticle and much to improve on immobilization methods. This thesis work is devoted to improving techniques for the quantification of protein immobilized on the gold nanoparticle and development of a novel approach to immobilize protein independent of pH.

The ability to evaluate antibody immobilization onto gold nanoparticles is critical for assessing coupling chemistry and optimizing the sensitivity of nanoparticle-enabled biosensors. Herein, we developed a fluorescence-based method for directly quantifying antibodies bound onto gold nanoparticles. Antibody-modified gold nanoparticles were treated with KI/I<sub>2</sub> etchant to dissolve the gold nanoparticles. A desalting spin column was used to recover the antibody released from the nanoparticles, and NanoOrange, a fluorescent dye, was used to quantify the antibody. We determined  $309 \pm 93$  antibodies adsorb onto each 60 nm gold nanoparticle ( $2.6 \times 10^{10}$  NP/mL), which is consistent with a fully adsorbed monolayer based on the footprint of an IgG molecule. Moreover, the increase in hydrodynamic diameter of the conjugated nanoparticle (76 nm) compared to that of the unconjugated nanoparticle (62 nm) confirmed that multilayers did not form. A more conventional method of indirectly quantifying the adsorbed antibody by

analysis of the supernatant overestimated the antibody surface coverage ( $660 \pm 87$  antibodies per nanoparticle); thus, we propose the method described herein as a more accurate alternative to the conventional approach.

The immobilization of antibody onto gold nanoparticles is important for many novel nanoparticle based immunoassays. Current methods of immobilization are limited by the inability to immobilize antibody onto gold nanoparticles over a range of pH values. Direct adsorption requires the pH to be slightly higher than the isoelectric point of the antibody and covalent attachment *via* bifunctional crosslinking chemistry molecules requires a specific pH as well. This is an issue when working with multiple antibodies at once for multiplex detection. In this thesis, we present a new method of immobilization by which the antibody is modified *via* a molecule with a *N*-hydroxysuccinimidyl ester group, then adsorbed onto a gold nanoparticle. We demonstrate that modification of antibodies allows for adsorption onto gold nanoparticles independent of pH. Furthermore, we show that this modification method is applicable to multiple antibodies. Finally, we show that these modified antibodies are active and comparable to conventional assays.

**KEYWORDS:** Antibody Conjugation, Antibody-Gold Nanoparticle Interactions, Protein Quantitation, Homogeneous Immunoassay, Fluorescence, DLS, NTA, Nanoparticle Aggregation

FORMATION, CHARACTERIZATION, AND OPTIMIZATION OF ANTIBODY-GOLD  
NANOPARTICLE CONJUGATES

SETH L. FILBRUN

A Thesis Submitted in Partial  
Fulfillment of the Requirements  
for the Degree of

MASTER OF SCIENCE

Department of Chemistry

ILLINOIS STATE UNIVERSITY

2017

© 2017 Seth L. Filbrun

FORMATION, CHARACTERIZATION, AND OPTIMIZATION OF ANTIBODY-GOLD  
NANOPARTICLE CONJUGATES

SETH L. FILBRUN

COMMITTEE MEMBERS:

Jeremy Driskell, Chair

Marjorie Jones

Christopher Mulligan

## ACKNOWLEDGMENTS

I would like to give a special thanks to my supervisor, Dr. Jeremy Driskell, for the encouragement, patience, and advice during my time as a graduate student in his lab. It has been a great ride as a graduate student in the Driskell lab.

I must thank Alex my fiancé for her continual support and encouragement throughout my time at ISU. I must also thank my family and friends for their love and care of my pursuit of a graduate degree in chemistry.

This work could not have been completed without the support of my fellow graduate students in the Department of Chemistry.

Finally, I must thank the faculty and staff of the Department of Chemistry for their endless provision of time and resources to push me to succeed.

S. L. F.

# CONTENTS

	Page
ACKNOWLEDGMENTS	i
CONTENTS	ii
TABLES	v
FIGURES	vi
CHAPTER	
I.    INTRODUCTION	1
Gold Nanoparticles (AuNP) for In-Vitro Diagnostics	1
Anatomy of Immunoglobulin G (IgG)	2
Immobilization of Protein onto AuNPs	4
Characterization of AuNP-Protein Conjugates	5
Coagulation Test for AuNP-Protein Stability	5
Light Scattering Techniques for AuNP-Protein Conjugation and Aggregate	
Detection	6
Dynamic Light Scattering	6
Nanoparticle Tracking Analysis	7
Protein Quantitation Methods for Protein-Conjugated AuNPs	8
Immunoassays Utilized in the Driskell Lab	9
Thesis Objective	12
Research Overview	12



II.	A FLUORESCENCE-BASED METHOD TO DIRECTLY QUANTIFY ANTIBODY IMMOBILIZED ON GOLD NANOPARTICLES	15
	Introduction	15
	Experimental	17
	Materials and Reagents	17
	Dissolution of Gold Nanoparticles	18
	Direct Determination of Antibody Surface Concentration	18
	Indirect Determination of Antibody Surface Concentration	19
	Instrumentation	20
	Nanoparticle Tracking Analysis (NTA)	20
	Flame Atomic Absorption Spectroscopy	20
	UV-Visible Absorption	21
	Fluorescence	21
	Results and Discussion	21
	Indirect Quantitation of Immobilized Antibody	21
	Dissolution of Gold Nanoparticles	24
	Direct Quantitation of Immobilized Antibody	27
	Effect of Coupling Chemistry on Immobilized Antibody	31
	Conclusions	32
III.	CHEMICAL MODIFICATION OF ANTIBODY ENABLES PH INDEPENDENT FORMATION OF STABLE ANTIBODY-GOLD NANOPARTICLE CONJUGATES	34
	Introduction	34
	Experimental	36

Materials	36
Antibody-NHS Modification	37
Protein Modified Gold Nanoparticles (pAuNPs)	37
Direct	37
DTSSP-Au	37
NHS-Antibody	38
Protein Modified AuNP Immunoassay	38
Direct	38
NHS-Antibody	39
Instrumentation	39
Dynamic Light Scattering	39
UV-Visible Absorption	39
Results and Discussion	40
Immobilization Methods	40
Acrylic Acid (NHS)	47
Amino Acid Analysis	53
Modified Antibody Functionality	54
Conclusions	59
IV. CONCLUSIONS AND FUTURE DIRECTIONS	60
Research Summary	60
Outlook and Future Directions	62
REFERENCES	64

## TABLES

Table	Page
1. Stability of goat anti-mouse IgG in 1 % (wt/v) NaCl solution using the varying conjugation techniques over a pH range of 6-8.5.	44
2. Stability of mouse anti-rabbit IgG in 1 % (wt/v) NaCl solution using the varying conjugation techniques at a pH range of 6-8.5.	50
3. Stability of rabbit anti-mouse IgG in 1 % (wt/v) NaCl solution using the varying conjugation techniques at a pH range of 6-8.5.	52
4. Hydrodynamic diameter ( $D_H$ ) increase of the DLS assay with acrylic acid (NHS) modified goat anti-mouse IgG at a pH range of 6.0-8.5, and direct adsorption at pH 8.5.	55
5. Figures of merit for the dynamic light scattering immunoassay with goat anti-mouse IgG comparing direct adsorption at pH 8.5 to acrylic acid (NHS) modified antibody at pH 6.5.	58

## FIGURES

Figure	Page
1. General structure of an IgG with the heavy chain colored in blue and the light chain colored in green.	3
2. Schematic of how intensity fluctuations are related to the Brownian motion of a particle in DLS.	6
3. A schematic of the NTA sample stage.	8
4. A) Schematic of antibody modified AuNPs before and after aggregation. B) Typical histogram observed with DLS on a negative control (PBS) and an antigen sample (5 ng/mL) with relative abundance vs hydrodynamic diameter (nm).	10
5. Schematic of ERL preparation and a SERS immunoassay.	11
6. An overview of the protein quantification process.	13
7. An illustration of the immobilization methods.	14
8. Size distribution of AuNP and antibody-modified AuNP measured with NTA.	22
9. Bio-Rad protein assay calibration curve for determining antibody concentration in AuNP supernatant.	23
10. Flame atomic absorption spectroscopy calibration curve for determining gold concentration.	25
11. Concentration of gold in 1 mL samples measured with flame atomic absorption spectroscopy.	26
12. Calibration curve for the NanoOrange-based fluorescence detection of antibody.	27
13. The absolute surface coverage of antibodies adsorbed onto 60 nm a AuNP measured with the fluorescence-based NanoOrange assay of the antibodies isolated from the	

AuNP (direct quantitation) and the Bio-Rad-based assay of excess unbound antibodies in the AuNP supernatant (indirect quantitation).	28
14. Nanoparticle size distribution curves for AuNP modified with varying amounts of antibody measured with NTA.	29
15. Saturation curves for the adsorption of antibody onto AuNPs.	30
16. Schematic of the types of immobilization methods.	41
17. Goat anti-mouse IgG functionalized gold nanoparticles by direct adsorption and by DTSSP functionalized gold nanoparticles before the addition of antibody.	42
18. DLS of antibody functionalized gold nanoparticles after the addition of NaCl.	43
19. Goat anti-mouse IgG modified with 0.5 mM DTSSP conjugated onto 60 nm gold nanoparticles.	46
20. Goat anti-mouse IgG modified with 0.5 mM acrylic (NHS) (top) and by direct adsorption (bottom) conjugated onto 60 nm gold nanoparticles.	48
21. DLS of mouse anti-rabbit IgG functionalized gold nanoparticles after the addition of NaCl.	49
22. DLS of rabbit anti-mouse IgG functionalized gold nanoparticles after the addition of NaCl.	51
23. Calibration curve of the DLS immunoassay with goat anti-mouse IgG showing the $D_H$ increase with respect to concentration of IgG.	55
24. Calibration curve of goat anti-mouse IgG with direct adsorption at pH 8.5 and acrylic acid modified at pH 6.5.	57
25. Calibration curve of acrylic acid (NHS) modified goat anti-mouse IgG at pH 6.5 with and without filtering <i>via</i> a spin column.	59

26. DLS with mean  $D_H$  increase vs IgG concentration comparing whole antibody vs Fab fragment.

63

## CHAPTER I

### INTRODUCTION

#### **Gold Nanoparticles (AuNP) for In-Vitro Diagnostics**

Gold nanoparticles (AuNPs) conjugated to various biomolecules utilized for diagnostic purposes have been a large area of interest in recent years. AuNPs are useful because they have unique physical and chemical properties that can be exploited for many enhanced chemical and biological detection techniques.<sup>1-3</sup> The surface chemistry of gold nanoparticles is readily tuned; thus, detection platforms utilize a variety of biomolecules that can be conjugated to AuNPs such as proteins, nucleic acids, and polysaccharides to facilitate the detection of a variety of analytes.<sup>2,3</sup> Several detection platforms capitalize on the unique optical properties of gold nanoparticles for signal transduction. Endo and co-workers used localized surface plasmon resonance (LSPR) to develop a nanoparticle-based chip capable of detecting multiple antibodies at once at a 100 pg/mL detection limit.<sup>4</sup> Elghanian *et al.* took advantage of nucleotide modified gold nanoparticles and developed a sensitive colorimetric platform for detection of polynucleotides with ~10 femtomolar detection limits.<sup>5</sup> Many groups have used dynamic light scattering (DLS), including the Driskell lab for the detection of influenza and the Huo group for the detection of cancer biomarkers, as a simple, one-step, and high throughput technique.<sup>6-9</sup> Surface enhanced Raman spectroscopy (SERS) is a widely known technique in which modified gold nanoparticles are used for the detection of many analytes at once.<sup>10-13</sup> Many diagnostic techniques employing metallic nanoparticles for the detection of specific biomarkers entail proteins to be adsorbed onto the surface of the nanoparticle due to the high specificity and selectivity of proteins. Antibody-antigen interactions are highly exploited in many of these detection techniques.<sup>11</sup> Consequently, conjugation is fundamental to the stability, functionality,

and overall success of AuNP based detection platforms. Similarly, efficiency of the conjugation chemistry, i.e., the number of adsorbed proteins, is imperative to the optimization of novel immunosensors.

### **Anatomy of Immunoglobulin G (IgG)**

It is vital to know the structure and function of the protein when developing an assay. The normal function of IgG antibodies is to bind to a specific target (antigen). IgGs are in the body to recognize many foreign objects such as proteins, bacteria, and viruses that are introduced into the body, and IgG is produced by b-cells as a secondary immune response to these foreign objects.<sup>14</sup>

IgG is a protein dimer made up of two main portions: the heavy chain and the light chain. The heavy chain is made up of three domains in the constant region  $C_{H1}$ ,  $C_{H2}$ , and  $C_{H3}$  and one variable region  $V_H$ ; each of these domains are approximately 110 amino acids in length.<sup>14</sup> The light chain is made up of two domains, a constant portion denoted as  $C_L$  and a variable portion  $V_L$ ; these domains are approximately 110 amino acids in length as well.<sup>14</sup> These can be further broken down into the Fc portion that consists of the  $C_{H2}$  and  $C_{H3}$  subunits and the Fab portion that consist of the  $C_{H1}$ ,  $V_H$ ,  $C_L$ , and  $V_L$  subunits.<sup>14</sup> The differences in the  $C_H$  domains typically affect the flexibility and affinity with antigens.<sup>15</sup> Figure 1 is a cartoon depiction of a typical IgG molecule.



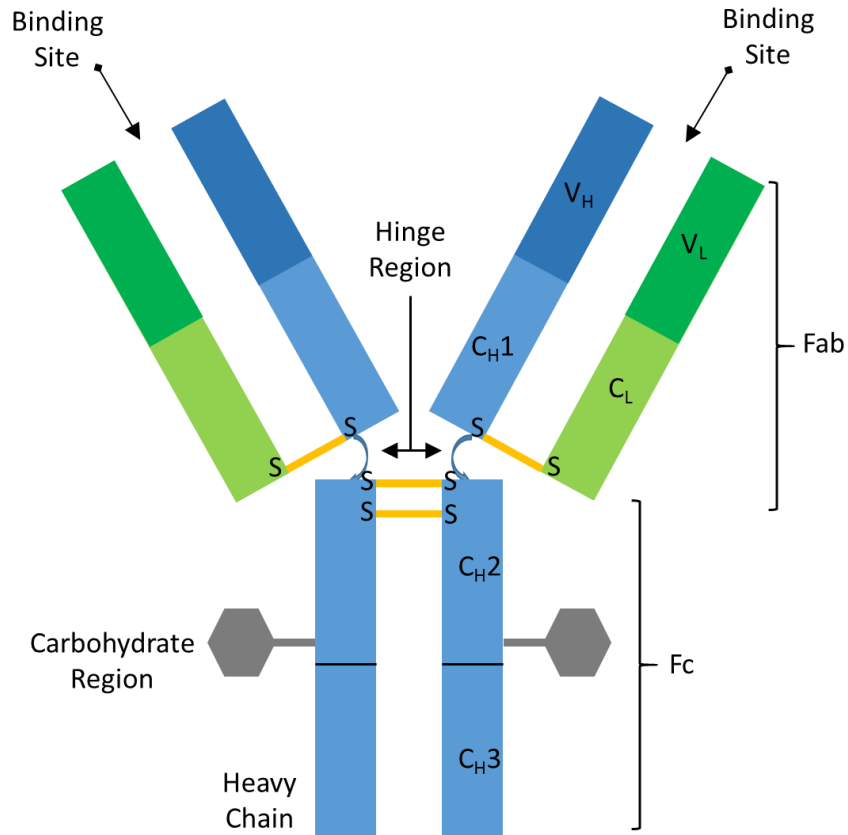


**Figure 1.** General structure of an IgG with the heavy chain colored in blue and the light chain colored in green. The darker colors indicate the variable regions of the light and heavy chains where the binding sites are located.

The Fc and Fab regions are held together by disulfide bonds; this is very important to the structure of the IgG protein.<sup>15</sup> In IgG, each subunit has at least one interchain disulfide bond and one holding the Fab heavy and light chains together. Also there are two disulfide bonds connecting the Fc portion to the Fab portion.<sup>14</sup>

The binding sites are located in the variable regions (V<sub>H</sub> and V<sub>L</sub>) on the Fab portion of the antibody with two identical binding sites per IgG molecule. On the Fc portion of the antibody there are a few N-linked glycans bonded *via* N-C bond on each of the C<sub>H</sub>2 domains; these

carbohydrates help with affinity toward binding to Fc receptors on the surface of cells such as T-cells.<sup>14</sup> While the function is largely unknown, it has been experimentally shown that without these glycans the Fc receptors do not bind with the same affinity.<sup>14</sup>

### **Immobilization of Protein onto AuNPs**

There are a variety of methods to immobilize protein onto AuNPs; however, they can be classified into two types of immobilization, non-covalent and covalent. Non-covalent attachment is simply the direct adsorption of protein onto gold nanoparticles. This attachment occurs through electrostatic and hydrophobic interactions between the protein and AuNP.<sup>16,17</sup> Direct adsorption has limitations due to the attachment requiring the pH of the solution to be specific for each protein. It has been shown that for optimal binding the solution pH must be slightly higher than the isoelectric point (pI) of the antibody.<sup>18</sup> Further limitations of direct adsorption include nonspecific adsorption and random orientation of the protein onto the surface of the gold nanoparticle.

In an effort to overcome the limitations of direct adsorption, several methods have been developed by which proteins can be covalently attached onto the surface of gold nanoparticles. Carbohydrates, if present on the protein, can be used for immobilization; however, this is a labor-intensive method which requires several steps and is time consuming.<sup>19</sup> One of the most common covalent immobilization strategies is the use of *N*-hydroxysuccinimidyl ester molecules for cross-linking proteins onto the surface of a gold nanoparticle.<sup>20</sup> This is performed by first covalently adding an *N*-hydroxysuccinimidyl ester molecule onto the surface of the gold nanoparticle, followed by the addition of the desired protein. The linking process has been thought to be performed by creating an amide bond through a terminal amine group presented by a lysine; however, recently it has been shown that hydrolysis of the ester groups occurs faster

than aminolysis of the amine to form an amide bond.<sup>21</sup> Proteins A and G can also be used to immobilize antibody onto the gold nanoparticle for directed immobilization.<sup>22</sup> These binding proteins have an affinity to the Fc region of IgG making them an ideal method of non-covalent conjugation; however, this binding occurs reversibly. Also, proteins A and G do not have the same affinity for all antibodies; thus, they cannot be applied as universal immobilization strategies. For example, protein A strongly binds human IgG but weakly binds to goat IgG.<sup>23</sup>

### **Characterization of AuNP-Protein Conjugates**

#### *Coagulation Test for AuNP-Protein Stability*

When developing a new nanosensor based on proteins conjugated onto gold nanoparticles it is important to confirm that the protein of interest attaches onto the nanoparticle. Additionally, it is necessary to establish that the protein-gold nanoparticle conjugate is stable under saline conditions. The necessity of a saline environment is important for the protein to function properly due to native physiological conditions of the protein. These two conditions can be evaluated with a simple coagulation study of the gold nanoparticle-protein conjugate of interest.<sup>24</sup> A coagulation test is the addition of NaCl into the solution of a gold nanoparticle-protein conjugate. Typically gold nanoparticles are citrate reduced; thus, the negatively charged citrate surrounds the positively charged gold nanoparticle forming an electrical double layer to stabilize AuNPs in solution.<sup>25</sup> Since NaCl is highly soluble in water, the Na<sup>+</sup> and Cl<sup>-</sup> ions will disrupt the electric double layer and cause AuNPs to aggregate. If a protein adsorbs onto the gold nanoparticles surface it will displace the citrate group leaving a stable conjugate (i.e. new electrical double layer); however, in the absence of full protein coverage this electrical double layer collapses causing aggregation. This aggregation, if significant, can be detected by the

naked eye. The native color of a 60 nm gold nanoparticle solution is red, but after aggregation it changes to blue-purple and even colorless if the aggregates are large enough to sediment.

## Light Scattering Techniques for AuNP-Protein Conjugation and Aggregate Detection

### *Dynamic Light Scattering*

Dynamic light scattering (DLS) is a technique that is capable measuring the hydrodynamic diameter ( $D_H$ ) of gold nanoparticles and AuNP-protein conjugates. This allows for the detection of aggregates that cannot be seen by the naked eye and allows for the monitoring of protein conjugation onto AuNPs. DLS is measured using a 532 nm laser and illuminating the sample. The sample (particle) scatters the light which is then detected. Because the particle has Brownian motion, over time the intensity of the scattered light fluctuates which is measured by the detector (Figure 2). This size measurement is obtained from the detection of light intensity fluctuations.

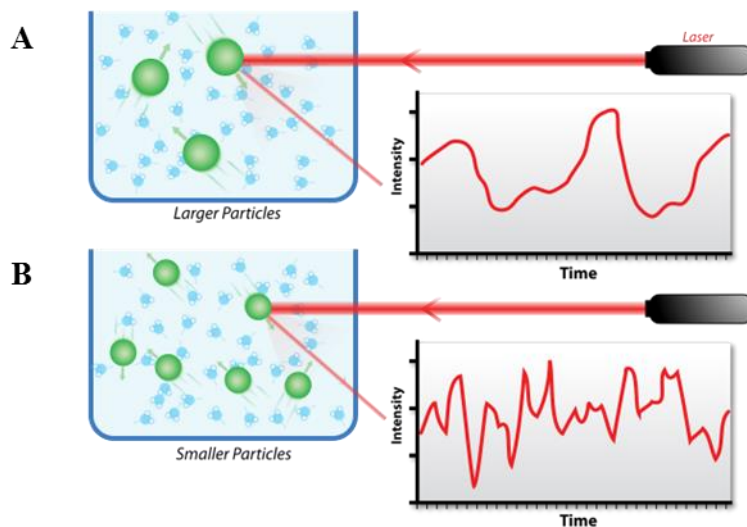


**Figure 2.** Schematic of how intensity fluctuations are related to the Brownian motion of a particle in DLS. A) Intensity fluctuations of a large particle. B) Intensity fluctuations of a small particle. Figure adapted from <https://en.wikipedia.org/wiki/File:DLS.svg>.<sup>26</sup>

If the particle is large, it will move slower thus the fluctuations in intensity over time will be broad as illustrated in Figure 2A. If the particle analyzed is small, it will be moving faster through solutions giving more fluctuation over time shown in Figure 2B. These fluctuations are fit to the auto correlation function to calculate D, which can be correlated to  $D_H$  via the Stokes-Einstein equation (Equation 1)

$$D_H = \frac{kT}{3\pi\eta D} \quad (1)$$

where  $D_H$  is the hydrodynamic diameter, k is the Boltzmann constant, T is temperature in Kelvin,  $\eta$  is the viscosity of the solution, and D is the translational diffusion coefficient.<sup>27</sup> DLS is a high throughput technique that is valuable for monitoring protein-AuNP interactions.

#### *Nanoparticle Tracking Analysis*

Another method of aggregate detection and protein conjugation onto AuNPs is nanoparticle tracking analysis (NTA). While NTA also measures the  $D_H$  of a gold nanoparticle-protein conjugate through the detection of scattering, it performs this by illuminating the sample with a 532 nm laser and measuring the scattered light by capturing a video via microscope focusing shown in Figure 3.<sup>28</sup>

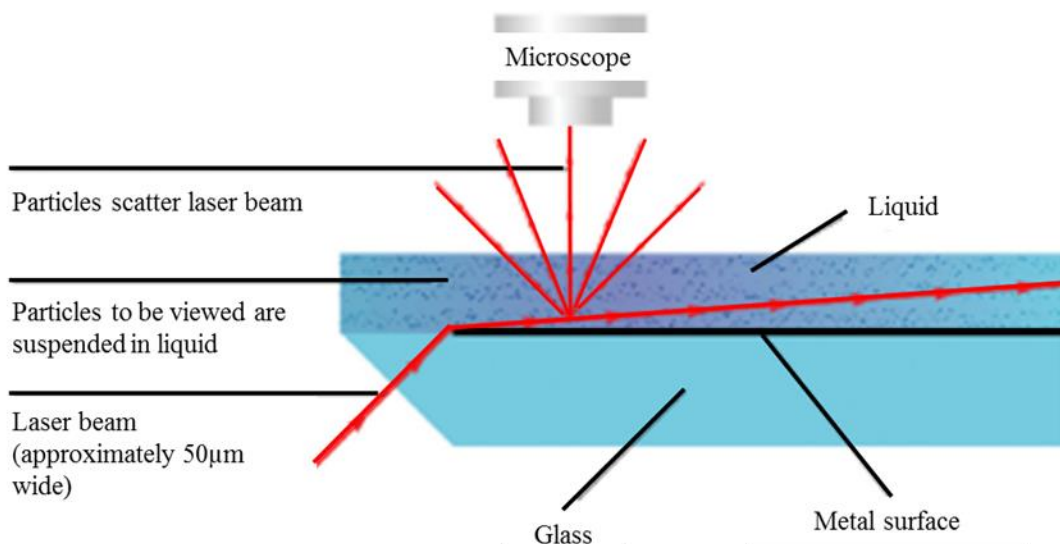


**Figure 3.** A schematic of the NTA sample stage. Adapted from (B. Carr *et al.*)<sup>28</sup>

The captured video is then analyzed with NanoSight software that correlates the particles' Brownian motion to the  $D_H$  utilizing the Stokes-Einstein equation (Equation 1). NTA calculates the  $D_H$  by tracking individual particles in the NanoSight software; this allows it to calculate the absolute number of particles analyzed giving rise to the concentration of particles in solution. Similar to DLS, NTA is a useful technique for the detection of antibody binding onto gold nanoparticles by measuring a shift in the hydrodynamic diameter of the nanoparticles before and after antibody conjugation.

### **Protein Quantitation Methods for Protein-Conjugated AuNPs**

When developing an immunosensor by immobilizing protein onto AuNPs, a method for the accurate quantitation of protein surface coverage is critical for the optimization of assay performance. Direct quantitative methods of measuring protein immobilized on the surface of AuNPs is challenging, regardless of this being fundamental to the development of novel AuNP based assays. Supernatant analysis of the excess protein after incubation with AuNPs by

modified Bradford or BCA total protein assays are the most common methods of approaching this problem.<sup>29,30</sup> For example Vertegel *et al.* determined there are 120 lysozyme molecules on a 20 nm silica nanoparticle using supernatant analysis with a BCA total protein assay.<sup>30</sup> These methods, however, are used to infer the amount of protein adsorbed onto AuNPs and are not a direct measurement. Pollitt *et al.* measured shifts in surface plasmon resonance due to protein adsorption as a tool to quantify the amount of antibody directly adsorbed onto a gold nanoparticle corresponding to 80 antibody molecules per 50 nm particle.<sup>31</sup> This is a direct method of analysis; however, it requires accurate knowledge of the refractive index at the gold nanoparticle surface. This is challenging since the refractive index is dependent on coverage, orientation, and water content, all of which are variable.<sup>31-33</sup> Other techniques such as dynamic light scattering (DLS)<sup>32,34,35</sup> and nanoparticle tracking analysis (NTA)<sup>7,32</sup> are used to monitor protein adsorption as a function of increasing protein-AuNP diameter, but they measure the surface coverage of protein and do not directly quantify the protein.

### **Immunoassays Utilized in the Driskell Lab**

Currently in the Driskell lab group we employ two methods for simple, fast, and specific detection of proteins: dynamic light scattering (DLS) and surface enhanced Raman spectroscopy (SERS).

The first method of detection used in our lab for immunoassays is a dynamic light scattering (DLS) assay. DLS measures the hydrodynamic diameter of a nanoparticle based on the Brownian motion of the nanoparticle.<sup>27</sup> This assay is a simple one-step method that is fast, sensitive, and accurate. In this method, antibody is immobilized onto a gold nanoparticle. When the antibody-modified gold nanoparticles are introduced to antigen they bind around it forming large aggregates as illustrated in Figure 4A.

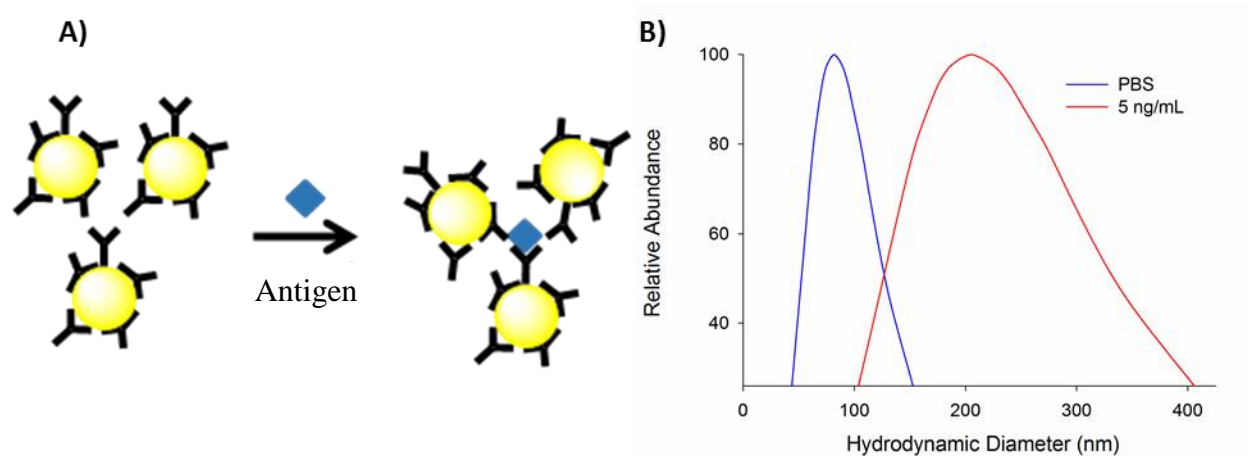


**Figure 4.** A) Schematic of antibody modified AuNPs before and after aggregation. B) Typical histogram observed with DLS on a negative control (PBS) and an antigen sample (5 ng/mL) with relative abundance vs hydrodynamic diameter (nm).

Prior to the addition of antigen, or in the case of a negative sample, a uniform narrow peak is observed indicating that the conjugates are not aggregated (Figure 4B). Upon mixing with antigen, the antibody modified gold nanoparticles aggregate and a large size increase is observed in the DLS histogram (Figure 4). Our group has previously demonstrated this DLS assay can be performed in 1 hour and provides a better detection limit than traditional ELISAs which require 24 hours to complete.<sup>6</sup>

Surface-enhanced Raman spectroscopy is a two-step immunoassay with gold nanoparticles that are co-functionalized with an antibody and a Raman reporter. These functionalized gold nanoparticles are commonly referred to as extrinsic Raman labels (ERLs) (Figure 5A). Similar to the DLS assay described above, this assay takes advantage of the high specificity of antibody-antigen interactions, and ERLs form large aggregates when antigen is introduced. These aggregates are captured on a 0.2  $\mu\text{m}$  polycarbonate tract etch (PCTE) filter



while the remaining unaggregated ERLs flow through the filter to waste (Figure 5B).<sup>11</sup> SERS is measured on the filter surface to determine the quantity of analyte. This method is fast, simple, and has the capability for the simultaneous detection of multiple analytes. In a multiplexed SERS assay, multiple ERLs are prepared, each with a different antibody and Raman reporter that has a unique spectrum for easy and fast identification.

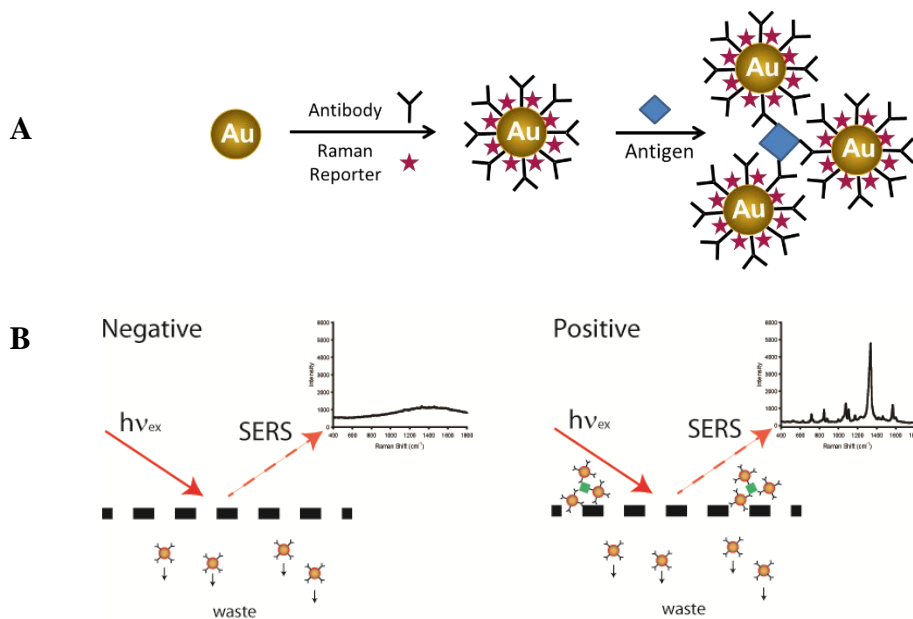


**Figure 5.** Schematic of ERL preparation and a SERS immunoassay. A) ERL preparation and aggregation. B) Typical SERS assay with the aggregates sticking on the filter while non-aggregated ERLs flow through the filter to waste.<sup>11</sup>

Central to both detection platforms, protein is immobilized onto the surface of gold nanoparticles. The previous work in the Driskell lab has established proof of principle for these two novel assays;<sup>6,11</sup> however, better characterization techniques of these conjugates are needed. For example, a long standing question is the absolute number of antibody adsorbed onto each nanoparticle. Moreover, greater efforts on conjugate chemistry are needed, particularly for the development of multiplexed assays. We have found that each antibody requires unique solution

conditions to remain stable.<sup>6</sup> Thus, the development of a synthetic approach to yield stable conjugates, independent of antibody, that can co-exist in a single solution is needed.

### **Thesis Objective**

Based on previous work done in the Driskell Lab as well as literature research, the focus of this thesis is to develop a method for the direct quantitation of protein adsorbed onto gold nanoparticles and to develop a technique to stabilize multiple unique Ab-AuNP conjugates in the same suspension.

### **Research Overview**

A fundamental aspect of preparing protein conjugated AuNPs for immunoassays is the ability to quantify the amount of antibody on the surface of the gold nanoparticle. This is a key element for the determination of the quality of the assay and for assay optimization. While there are methods of quantifying antibody such as supernatant analysis which can be used to infer the amount of protein adsorbed *via* modified Bradford assays or BCA total protein assays,<sup>29,30</sup> these methods are indirect and do not measure the exact amount of protein adsorbed onto the AuNP. Therefore, we developed and evaluated a novel scheme (Figure 6) to isolate and detect the antibodies adsorbed onto the AuNP as an improved method to accurately and quantitatively determine the number of antibodies per AuNP.

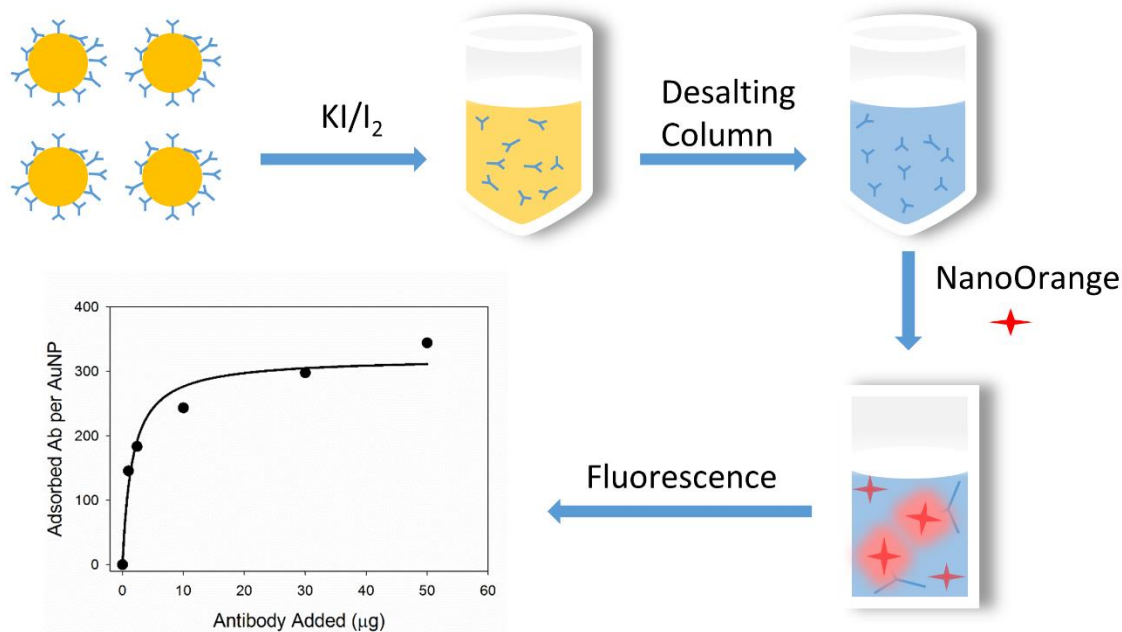


**Figure 6.** An overview of the protein quantification process.

Protein modification of gold nanoparticles is essential for many novel nanoparticle based immunosensors including those currently under development in the Driskell lab. Procedures can have many steps or be as simple as directly adsorbing protein onto AuNPs; however, most procedures have one common drawback, the inability of the immobilization process to produce stable AuNP-protein conjugates under a range of pH values. This is problematic because all proteins have a specific pH at which they can be immobilized which is slightly more basic than the isoelectric point of the protein.<sup>18</sup>

Conventional methods of immobilization are performed by direct adsorption presented in Figure 7A or with a bifunctional crosslinking molecule such as 3, 3'-dithiobis(sulfosuccinimidyl propionate) (DTSSP) shown in Figure 7B.

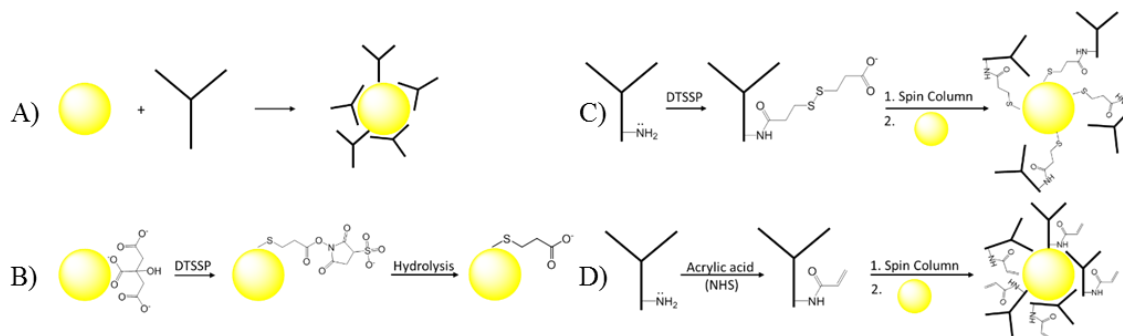


**Figure 7.** An illustration of the immobilization methods. A) Direct adsorption. B) Immobilization utilizing DTSSP as a bifunctional crosslinking molecule. C) Method of immobilization by attaching DTSSP to the antibody before adsorbing onto the AuNPs. D) Method of immobilization by attaching to acrylic acid (NHS) onto the antibody before adsorbing onto the AuNPs.

Recent studies suggest that hydrolysis occurs faster than aminolysis; thus, conventional methods of immobilization using a bifunctional crosslinking molecule do not produce stable antibody-AuNP conjugates over a range of pH values. If bifunctional crosslinking is attempted *via* the addition of DTSSP on the nanoparticle surface then it requires the antibody to diffuse through the solution to come into contact with the DTSSP before hydrolysis occurs of the terminal ester group on the DTSSP molecule (Figure 7B). In this work, we used the bifunctional crosslinking molecule (DTSSP) that is conventionally used; however, we modified the antibody before the introduction of AuNPs (Figure 7C). This modification allowed for the concentration and diffusion rate of the DTSSP molecule to facilitate aminolysis with the terminal amine of lysine before hydrolysis of the hydroxysuccinidyl ester group on DTSSP. Finally we used acrylic acid (NHS) (Figure 7D) to determine if the terminal sulfur group facilitates binding to AuNPs.

## CHAPTER II

### A FLUORESCENCE-BASED METHOD TO DIRECTLY QUANTIFY ANTIBODY IMMOBILIZED ON GOLD NANOPARTICLES

This Study has been published in the journal *Analyst* as Seth L. Filbrun and Jeremy D. Driskell.

A fluorescence-Based Method to Directly Quantify Antibodies Immobilized on Gold Nanoparticles. *Analyst*. **2016**, 141, 3851-3857. <sup>36</sup>

#### **Introduction**

Protein-modified gold nanoparticles are central to many novel and emerging biosensing technologies.<sup>37-40</sup> The sensitivity of these nanoparticle-based methods is often governed by the coupling chemistry between the nanoparticle and protein; an interaction which controls the surface coverage and protein orientation.<sup>3,41-43</sup> In order to optimize the surface coupling chemistry and increase assay performance, a method for the accurate quantitation of surface coverage is critical. Such a method will enable conditions for maximum protein coverage to be identified, and facilitate proper assessment of novel coupling chemistry by ensuring enhanced assay performance is due to improved orientation rather than surface coverage. In addition, an accurate method to quantify surface coverage is needed to assess the reproducibility of nanoparticle preparations which can influence assay quality control.<sup>43</sup>

Direct quantitative methods to measure surface coverage of proteins conjugated onto gold nanoparticles remains challenging, despite this being of fundamental importance to nanoparticle-based applications. Most commonly, analysis of excess protein in the supernatant after incubation with the nanoparticle suspension is used to infer the quantity of adsorbed protein. Protein concentrations are often low; but, modified Bradford and BCA total protein assays are typically capable of detecting these low concentrations.<sup>30,44</sup> Alternatively, fluorescently labelled

proteins can be used and low concentrations of excess proteins in solution can be measured with fluorescence.<sup>45,46</sup> This requires modification of the protein by fluorophore functionalization, which can interfere with the coupling chemistry or affect the protein adsorption characteristics. These approaches are indirect measurements of the adsorbed protein and assume no loss of protein due to adsorption to container walls, e.g., centrifuge tube. Nevertheless, this approach results in a measure of the absolute number of immobilized antibodies per nanoparticle.

More recently, antibody adsorption has been quantified by measuring shifts in the surface plasmon resonances due to changes in the local refractive index caused by protein adsorption.<sup>31</sup> While this is a more direct analysis of the adsorbed proteins, it requires accurate knowledge of the refractive index at the nanoparticle surface. This is quite challenging considering the refractive index depends on coverage, orientation, and water content, none of which are constant.<sup>47-49</sup>

A number of additional techniques have been evaluated to measure the surface concentration relative to saturation, but do not give an absolute quantitation of adsorbed protein. Dynamic light scattering (DLS)<sup>7,47,50,51</sup> and nanoparticle tracking analysis (NTA)<sup>7,47</sup> measure an increase in hydrodynamic diameter upon protein adsorption. The increase in diameter is correlated with relative surface coverage. Similarly, zeta potential,<sup>52,53</sup> analytical ultracentrifugation,<sup>54</sup> and electrospray differential mobility analysis<sup>55</sup> have all been used to measure relative surface coverage.

In this chapter we present a fluorescence-based method for directly quantifying the absolute number of antibodies adsorbed onto gold nanoparticles. The detection of adsorbed antibodies is accomplished by dissolving the gold nanoparticle and using a fluorescent dye, NanoOrange,<sup>56,57</sup> to quantify the protein previously adsorbed onto the nanoparticles. A

fluorescent dye, such as NanoOrange, was selected to quantify the protein because fluorescence typically provides a lower detection limit and larger dynamic range than absorbance based protein quantification strategies. NanoOrange was specifically selected as the fluorescent dye as it has previously been demonstrated to broadly react with many proteins and has been well-characterized with respect to the effects of contaminants on assay performance.<sup>56</sup> We demonstrate that this novel method is more accurate than the commonly used indirect method based on mass difference in the added and excess antibody remaining in solution. To further demonstrate the utility of the method, we compare the surface coverage of antibody using two methods of immobilization, direct adsorption and DTSSP coupling chemistry.

## **Experimental**

### *Materials and Reagents*

Gold nanoparticles (AuNPs; 60 nm) were purchased from Ted Pella Inc. (Redding, CA). Iodine (99.8%, ACS reagent) and potassium iodide were purchased from Fisher Scientific (Waltham, MA). Borate buffer, goat anti-mouse IgG polyclonal antibody, 3,3'-dithiobis[sulfosuccinimidylpropionate] (DTSSP), NanoOrange protein quantitation kit, and Zeba spin desalting columns (7K MWCO, 0.5 mL) were obtained from Thermo Scientific (Rockford, IL). Gold(III) chloride hydrate (99.999% trace metals basis) was acquired from Sigma Aldrich (St. Louis, MO). Bio-Rad protein assay dye reagent concentrate was attained from Bio-Rad Laboratories, Inc. (Hercules, CA). All aqueous solutions were prepared in NANOpure deionized water (18 M $\Omega$ ) from a Barnstead water purification system (Thermo Scientific, Rockford, IL).

### *Antibody-Conjugated Gold Nanoparticles*

To directly adsorb antibody onto AuNPs, 1 mL of 60 nm AuNPs was placed into a microcentrifuge tube, then 40  $\mu$ L of 50 mM borate buffer (pH 8.5) was added to adjust the pH of

the solution to 8.5. Then 30  $\mu\text{g}$  of goat anti-mouse IgG was added, and the solution was incubated at room temperature for  $> 2$  hrs. After incubation the functionalized AuNPs were centrifuged at 12,500g for 5 min, the supernatant was decanted, and the pelleted nanoparticles were resuspended in 2 mM borate buffer. The centrifugation/resuspension process was repeated twice to thoroughly remove excess antibody.

Antibody was also immobilized onto AuNPs via DTSSP, a bifunctional coupling reagent. To this end, 1 mL of 60 nm AuNPs was placed into a microcentrifuge tube, then 40  $\mu\text{L}$  of 50 mM borate buffer (pH 8.5) was added to adjust the pH of the solution to 8.5, and 10  $\mu\text{L}$  of 5 mM DTSSP was added to the solution. After incubation at room temperature for 15 min the solution was centrifuged at 5,000g for 5 min. The supernatant was removed and the pelleted AuNPs were resuspended in 2 mM borate buffer (pH 8.5). The centrifugation/resuspension steps were repeated twice to ensure complete removal of excess DTSSP. To the DTSSP-modified AuNP, 30  $\mu\text{g}$  of goat anti-mouse IgG was added and allowed to incubate at room temperature for  $> 4$  hrs. The functionalized AuNPs were then centrifuged at 12,500g for 5 min and the pelleted AuNP resuspended in 2 mM borate buffer three times.

#### *Dissolution of Gold Nanoparticles*

AuNPs (1 mL) were dissolved by adding 50  $\mu\text{L}$  of a KI/I<sub>2</sub> solution consisting of 333 mM KI and 50 mM I<sub>2</sub>. This mixture was allowed to react for 15 min to ensure full dissolution of the AuNPs. Flame atomic absorption spectrophotometry was used to confirm the AuNPs were completely dissolved.

#### *Direct Determination of Antibody Surface Concentration*

NanoOrange reagent was prepared according to the manufacturer's protocol. Antibody functionalized AuNPs were centrifuged at 12,500g for 5 min, the supernatant was discarded and



50  $\mu\text{L}$  of KI/I2 solution was added according to the above procedure to dissolve the AuNPs. Standard solutions of goat anti-mouse IgG were prepared with appropriate steps to match the matrix of the samples. To prepare the standard solutions, 1 mL 60 nm AuNPs were centrifuged at 12,500g for 5 min, the supernatant was discarded, KI/I2 was added to the sedimented AuNP pellet, and the appropriate amount of antibody was then added to each standard. Desalting columns were used to remove the KI/I2 solution before using the NanoOrange reagent. The volume of antibody recovered from the desalting column was measured and NanoOrange reagent was added to each solution to bring the total volume to 1.5 mL. The samples were incubated for 20 min at 90° C in a water bath and cooled to room temperature in the dark. Fluorescence of the protein-bound NanoOrange dye was measured and correlated with antibody concentration.

#### *Indirect Determination of Antibody Surface Concentration*

Antibody functionalized AuNPs were centrifuged at 12,500g for 5 min and 500  $\mu\text{L}$  of the supernatant was analyzed using a modified Bradford assay (Bio-Rad protein assay). The collected supernatant was diluted 1:1 with 2 mM borate buffer (pH 8.5) and 250  $\mu\text{L}$  of the Bio-Rad reagent was added. Standard solutions of antibody (1- 20  $\mu\text{g}/\text{mL}$ ) were prepared in 2 mM borate buffer (pH 8.5) and 250  $\mu\text{L}$  of Bio-Rad reagent was added to 1 mL of each standard solution. The samples and standards were then incubated at room temperature for 15-20 min to allow the color to develop. Absorption was measured at 595 nm to quantify antibody in the supernatant. The absolute concentration of antibody adsorbed onto the AuNP was inferred to be the mass difference between the antibody added to the AuNP and the antibody remaining in the supernatant.

## Instrumentation

### *Nanoparticle Tracking Analysis (NTA)*

The hydrodynamic diameter of the functionalized AuNPs was measured using a NanoSight LM10, furnished with a temperature controlled LM14G sample viewing cell configured with a 532 nm laser (Malvern Instruments Ltd Worcestershire, UK). Tracking of the AuNPs was performed using a high sensitivity sCMOS camera (Hamamatsu Photonics). Samples were diluted 100-fold to  $\sim 10^8$  NP/mL and then injected with a 1 mL syringe (Becton Dickinson, NJ) utilizing a Harvard Apparatus Pump 11 Elite single injection syringe pump (Harvard Bioscience Inc. Holliston, MA). Flow injection rate was set to 15  $\mu$ L/min. Sample analysis was performed using NanoSight 2.3 software. The software was set to live mode with the camera level set to 6 and the detection threshold at 5. The samples were analyzed until greater than 10,000 completed tracks were acquired, and hydrodynamic diameter was calculated using the NanoSight 2.3 software.

### *Flame Atomic Absorption Spectroscopy*

The concentration of Au in the dissolved AuNPs was measured using an AAnalyst 200 Atomic Absorption Spectrometer furnished with an Au-Ag hollow cathode lamp (PerkinElmer Inc. Waltham, MA). Air was used as the oxidant at a flow rate of 12 L/min while acetylene was used as the fuel with a flow rate of 1.9 L/min. The Au absorption line at 242.80 nm was measured with a slit set to 2.7 mm x 1.35 mm. Samples were prepared by dissolving 1 mL of 60 nm AuNPs with 50  $\mu$ L of KI/I<sub>2</sub> solution and diluting to 10 mL with nanopure H<sub>2</sub>O.

### *UV-Visible Absorption*

UV-Visible absorption was performed using an Agilent 8453 spectrophotometer equipped with a photodiode array providing a spectral range of 190-1100 nm (Agilent Technologies Santa Clara, CA). Sample absorption was measured at 595 nm using 2 mM borate buffer (pH 8.5) as the blank.

### *Fluorescence*

Fluorescence spectra were acquired with a PerkinElmer LS 55 Luminescence Spectrometer (PerkinElmer Inc. Waltham, MA). Samples were excited at 485 nm and emission was measured at 590 nm, as recommended by the manufacturer's protocol for NanoOrange. Spectra were collected with 5 s integrations and the excitation/emission slit widths were maximized (15 nm/20 nm) to maximize the signal-to-noise ratio.

## **Results and Discussion**

### *Indirect Quantitation of Immobilized Antibody*

It is well-established that antibodies self-assemble onto the surface of AuNPs. Protein adsorption arises from a combination of electrostatic and hydrophobic interactions and is influenced by many parameters, including pH, ionic strength, and antibody pI.<sup>58-60</sup> Based on previously optimized conjugation conditions, antibody-modified gold nanoparticles were prepared by adding 30  $\mu$ g of goat anti-mouse IgG antibody to AuNPs.<sup>7</sup> NTA was performed on the unconjugated and antibody-modified AuNPs in order to confirm adsorption of antibody onto the AuNPs and the size distributions are shown in Figure 8. From the representative histograms in Figure 8, the unconjugated AuNPs had a mean hydrodynamic diameter of 62 nm while the modified AuNPs had a mean hydrodynamic diameter of 78 nm. The histograms shown in Figure 8 illustrate uniform size distributions of the NPs consistent with a monodisperse population.

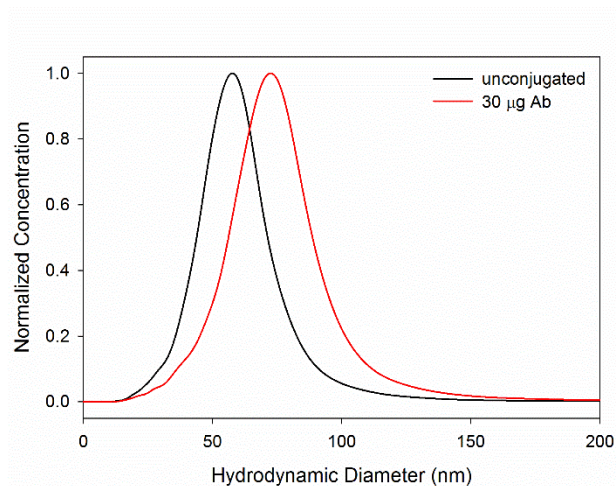


**Figure 8.** Size distribution of AuNP and antibody-modified AuNP measured with NTA. Greater than 10,000 particles were tracked to create each of the histograms.

NTA analysis of four additional preparations of unconjugated and antibody-modified AuNP produced similar histograms with a standard deviation of  $\pm 0.6$  nm in the mean diameter. The 16 nm shift in the mean diameter of the AuNPs upon conjugation of the antibody is consistent with other reports for nanoparticles fully saturated with protein.<sup>7,47,50,51</sup> The size of an IgG molecule has been previously reported as 4-10 nm depending on orientation;<sup>7,49,61,62</sup> and the 16 nm shift in the mean diameter of the AuNPs upon conjugation of the antibody is consistent with a monomolecular layer of adsorbed protein, although the possibility of a bilayer exists depending on antibody orientation. Recent work has demonstrated that protein monolayers form on nanoparticles,<sup>50,63,64</sup> although the possibility for additional proteins to adsorb do exist when excessively high solution concentrations of protein are used<sup>50</sup> or when the pH is near the protein isoelectric point.<sup>65</sup> Based on these previous works and our experimental conditions, we speculate that a protein monolayer is more likely than a bilayer.

The quantity of adsorbed protein was indirectly determined by analysis of excess antibody in the modified AuNP supernatant. A Bio-Rad protein assay was calibrated using standard solutions of goat anti-mouse IgG antibody (Figure. 9).

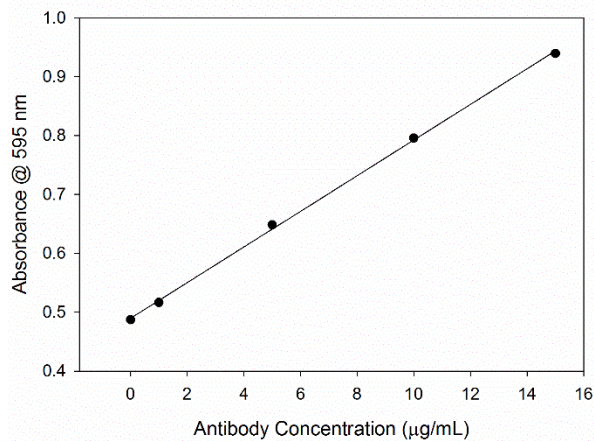


**Figure 9.** Bio-Rad protein assay calibration curve for determining antibody concentration in AuNP supernatant.

We determined that  $25.7 \pm 0.6 \mu\text{g}$  of antibody remained in the supernatant based on the analysis of supernatant from nine independent preparations of antibody-modified AuNP. It is inferred that  $4.3 \pm 0.6 \mu\text{g}$  of antibody adsorbed onto the AuNPs from the mass difference relative to the  $30 \mu\text{g}$  of antibody added to the AuNPs. This mass corresponds to the adsorption of  $660 \pm 87$  antibodies per AuNP. A conservative estimate of theoretical monolayer surface coverage is calculated to be 314 antibodies per AuNP based on the total surface area of the AuNPs ( $2.6 \times 10^{10}$  NP/mL at 62 nm) and assuming a 7 nm circle as the projected footprint of an antibody. Therefore, this method of quantifying antibody loading suggests multilayers of protein adsorbed onto the AuNP. This result, however, contradicts the speculation that a monolayer forms based on the NTA results (Figure 8) and previous works<sup>7,47,50,51</sup> as discussed above.

We hypothesized that loss of antibody due to adsorption to the centrifuge tube during AuNP modification would decrease the concentration of antibody in the supernatant and result in an overestimation of antibody adsorbed onto the AuNP. To test this hypothesis, 30  $\mu\text{g}$  of antibody was added to 1 mL of 2 mM borate buffer (pH 8.5) in a microcentrifuge tube. The solution was incubated for 2 hours at room temperature and centrifuged, the same conditions used for AuNP modification. The protein solution was then analysed with the Bio-Rad protein assay and  $27.5 \pm 0.3 \mu\text{g}$  of protein were recovered, based on three independent analyses, which suggested that  $2.5 \pm 0.3 \mu\text{g}$  were adsorbed onto the surface of the centrifuge tube. Accounting for the loss of antibody adsorbed onto the centrifuge tube, we can estimate that only 1.8  $\mu\text{g}$  of the 4.3  $\mu\text{g}$  mass difference determined above was due to adsorption onto AuNP. This adsorbed mass corresponds to a surface coverage of 280 antibodies per AuNP, which further supports our claim of monolayer coverage.

These studies established that the common method of quantifying antibody adsorbed onto AuNPs by mass difference leads to an overestimation of the surface coverage. While we show it may be possible to understand the source of and correct for this systematic bias, these corrective procedures will increase the uncertainty in the measured values. It is clear that an improved analytical method that directly measures the adsorbed antibodies is needed.

#### *Dissolution of gold nanoparticles*

The dissolution of AuNPs is central for the direct analysis of antibodies adsorbed to the surface of the AuNP. To this end AuNPs were dissolved by adding a well-established iodine-iodide etchant solution to dissolve 1 mL of 60 nm AuNPs. The Au is dissolved by the oxidant ( $\text{I}_3^-$ ) which is formed through the reaction of  $\text{I}_2$  and  $\text{I}^-$ .<sup>66</sup>

Flame atomic adsorption spectroscopy was used to confirm that the AuNPs were fully dissolved by the KI/I<sub>2</sub> etchant solution. A calibration curve for the quantitation of Au was constructed using standard solutions prepared from gold (III) chloride (Figure 10).

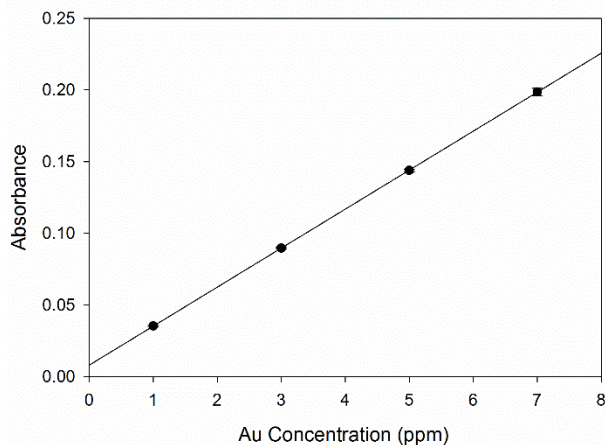


**Figure 10.** Flame atomic absorption spectroscopy calibration curve for determining gold concentration.

A 1 mL sample of AuNPs was centrifuged and the supernatant was analysed for Au. Figure 11 shows that no gold was detected in the supernatant which confirms that all of the AuNPs were pelleted upon centrifugation and that the gold ions used to synthesize the AuNPs were fully reduced during preparation. The pelleted AuNPs were then dissolved with the addition of 50  $\mu$ L of KI/I<sub>2</sub>, and  $51.1 \pm 0.4 \mu$ g of gold were measured in this sample with flame AA (Figure 11).

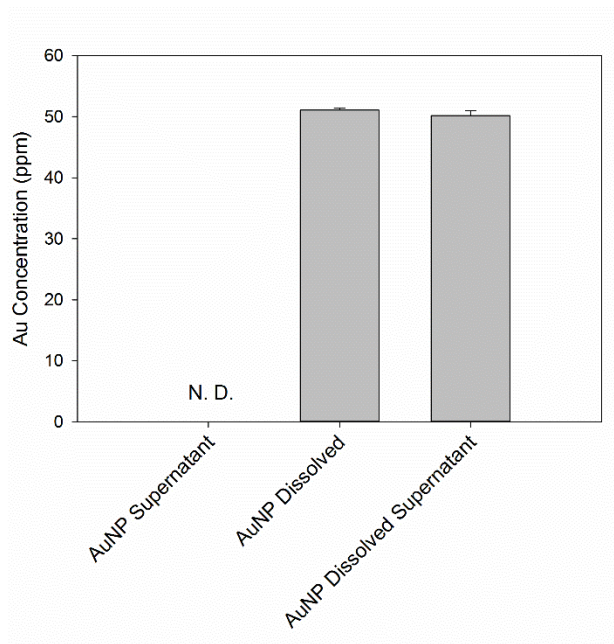


**Figure 11.** Concentration of gold in 1 mL samples measured with flame atomic absorption spectroscopy. The concentrations are calculated from the average of three measurements and the error bars represent the standard deviation. (N. D. = not detected).

The theoretical value of Au in 1 mL of AuNPs is 51  $\mu\text{g}$  calculated using the concentration provided by the manufacture ( $2.6 \times 10^{10}$  NP/mL) and the hydrodynamic diameter of the unconjugated AuNPs measured by NTA (Figure 8). The statistically equivalent values for the experimental and theoretical amounts of gold suggest that the AuNPs were fully dissolved. To further verify complete dissolution of the AuNP, the KI/I<sub>2</sub> treated AuNPs, i.e., dissolved AuNPs, were centrifuged to form a pellet of any remaining AuNPs on the bottom of the centrifuge tube. Although no pellet was visible, the “supernatant” was analysed and determined to contain  $50.2 \pm 0.8 \mu\text{g}$  of gold (Figure 11). Given that the amount of gold did not significantly decrease as a result of centrifugation after KI/I<sub>2</sub> treatment, it was concluded that the AuNPs were fully dissolved.



### *Direct Quantitation of Immobilized Antibody*

The AuNP core of the antibody-modified AuNP was fully dissolved as described above for the direct analysis of adsorbed antibodies, and a fluorescent dye, NanoOrange, was used to label the free protein for quantitation. However, when used in the solution that contains KI/I<sub>2</sub> there is interference with the fluorophore resulting in no detectable fluorescence. To circumvent this issue, a spin desalting column was used to remove excess KI/I<sub>2</sub>. After desalting, the isolated antibody was labelled with the fluorescent dye for quantitation.

In order to build an accurate calibration curve, the standard solutions were prepared in the same matrix as the sample and passed through a desalting column. These standards were prepared by centrifuging 1 mL of 60 nm AuNPs and dissolving the pellet with the KI/I<sub>2</sub> solution identical to the samples. Varying amounts of antibody were added to each solution and then the solution was passed through a desalting column to remove any salts that interfere with the interaction between NanoOrange and the antibody. The calibration curve for the NanoOrange-based assay is shown in Figure 12.

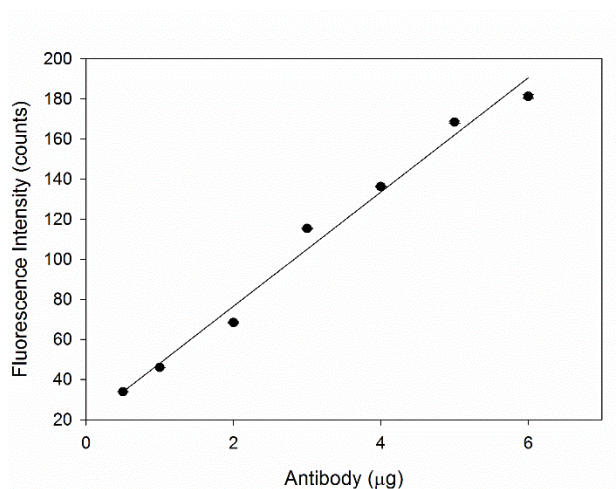


**Figure 12.** Calibration curve for the NanoOrange-based fluorescence detection of antibody. The samples were excited at 485 nm and the emission was measured at 590 nm.  $R^2 = 0.9925$ .

Direct analysis of antibody isolated, i.e., dissolved with KI/I<sub>2</sub> and desalted, from antibody-modified AuNP with the fluorescence assay measured a surface coverage of  $309 \pm 93$  antibodies per AuNP based on nine independent sample preparations (Figure 13). This is in contrast to the indirect method based on mass difference between added and excess antibody described above, which estimated  $660 \pm 87$  antibodies per AuNP (Figure 13).

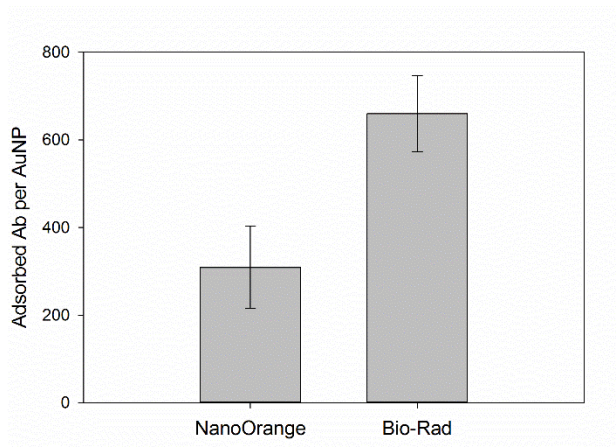


**Figure 13.** The absolute surface coverage of antibodies adsorbed onto a 60 nm AuNP measured with the fluorescence-based NanoOrange assay of the antibodies isolated from the AuNP (direct quantitation) and the Bio-Rad-based assay of excess unbound antibodies in the AuNP supernatant (indirect quantitation). Each bar represents the average surface coverage determined from nine independent preparations of modified AuNP and the error bars represent the standard deviation.

A t-test was performed to compare the direct and indirect methods of quantifying immobilized protein, and it was concluded with 99 % confidence that the surface coverages calculated with the two assays are significantly different. Notably, the surface coverage measured with this novel

fluorescence-based protocol is more consistent with both the NTA data that indicated a monolayer of adsorbed protein and the theoretical surface coverage of a protein monolayer.

To further validate the capability of this method to directly quantify immobilized antibodies, AuNPs were incubated with varying amounts of antibody. NTA was performed to characterize the antibody adsorption isotherm (Figure 14, Figure 15).

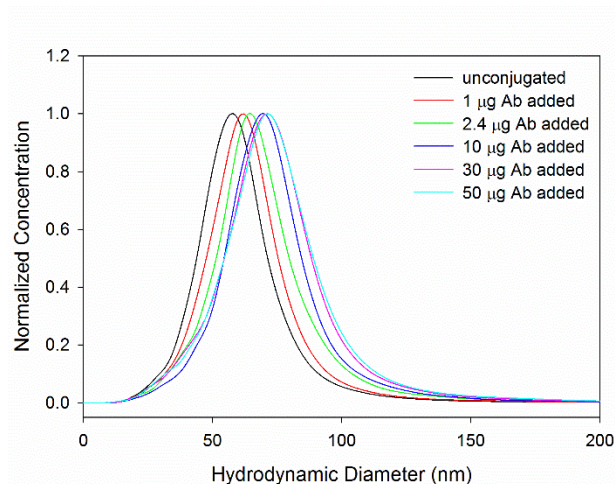


**Figure 14.** Nanoparticle size distribution curves for AuNP modified with varying amounts of antibody measured with NTA.

As is evident, the mean hydrodynamic diameter increased from 62 nm for the unconjugated AuNP to a maximum of 76 nm with increasing amounts of added antibody. Based on the NTA measured hydrodynamic diameter, the addition of antibody in excess of 10 µg did not result in increased surface coverage.

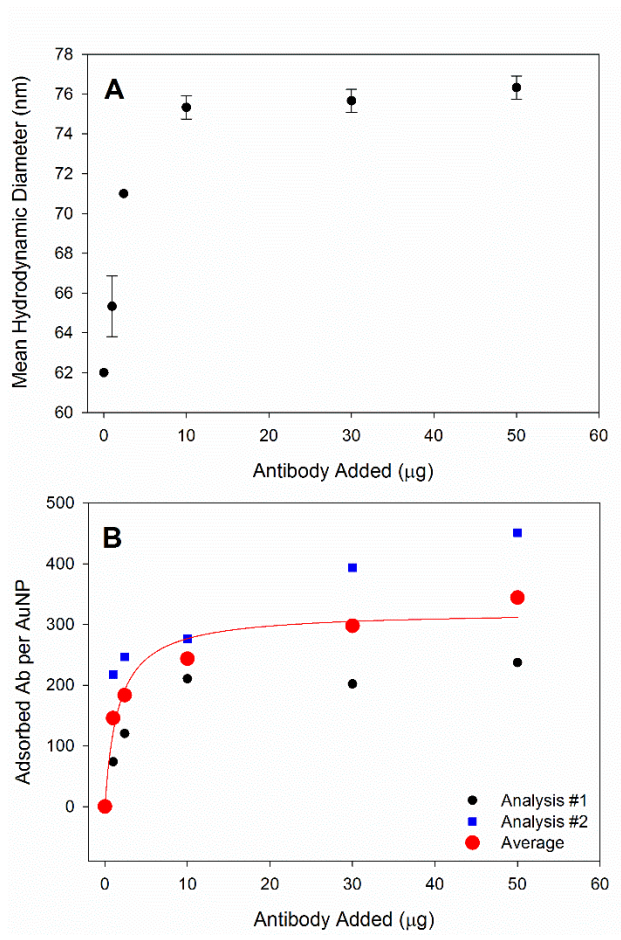


**Figure 15.** Saturation curves for the adsorption of antibody onto AuNPs. A) Increase in hydrodynamic diameter measured with NTA. B) Increase in absolute antibody surface coverage measured with the fluorescence-based method. Two independent analyses were performed to generate the fluorescence-based data and the average of the two runs was fit to Equation 2.

The antibody adsorption isotherm was also constructed using the absolute quantity of adsorbed antibody measured with the fluorescence method (Figure 15B). The analysis was performed twice and the average surface coverage was best fit to a ligand binding model (Equation 2).

$$y = \frac{B_{max}x}{K_d+x} \quad (2)$$

$B_{\max}$  is the maximum antibody surface coverage at saturation and  $K_d$  is the apparent dissociation constant. Based on the best fit curve, the surface coverage maximized at 323 antibodies per AuNP. This surface coverage is consistent with the value measured for nine independent preparations with 30  $\mu\text{g}$  antibody (Figure 13) and the theoretical value calculated from surface area (314 antibodies per AuNP). It is worth noting that the antibody surface concentration exceeds that of a monolayer for the two highest antibody concentrations for the second analysis (Figure 15B). While these measured values are not statistically different than monolayer coverage based on the precision of the fluorescence-based method, it is not possible to rule out the possibility of additional antibody molecules adsorbing to begin forming a multilayer when large concentrations of excess antibody are used.<sup>50</sup> These results further validate the fluorescence-based method and demonstrate that the method can be used to quantify sub-saturation coverages.

#### *Effect of Coupling Chemistry on Immobilized Antibody*

To explore the scope of this analytical method, we quantified antibody coupled to AuNPs through a bifunctional crosslinker, DTSSP.<sup>67,68</sup> A self-assembled monolayer was first formed on the AuNP surface through cleavage of the disulphide bond and formation of a gold-thiolate bond. Antibody was then added and primary amines from lysine residues reacted with the terminal succinimidyl ester to covalently immobilize the antibody through the formation of an amide bond. A recently published study suggests that DTSSP coupling chemistry is inefficient.<sup>21</sup> A detailed investigation of reaction kinetics determined that heterogeneous hydrolysis of the succinimidyl ester is three orders of magnitude greater than that of the heterogeneous aminolysis rate.<sup>21</sup> Thus, it is important to determine the effect of DTSSP coupling chemistry on antibody loading.

The DTSSP/antibody functionalized AuNPs were dissolved in KI/I<sub>2</sub> solution, desalted, and the isolated protein was quantified with NanoOrange. A total of  $1.9 \pm 0.3 \mu\text{g}$  were recovered from the surface of the functionalized AuNPs (N = 3 independent preparations), which corresponds to the coupling of  $298 \pm 46$  antibodies per AuNP. Thus, the surface coverage of antibody immobilized via DTSSP did not significantly differ from the surface coverage obtained via direct adsorption of antibody to the AuNP ( $309 \pm 94$  antibodies per AuNP). Hydrolysis of the DTSSP-modified AuNP results in surface-bound carboxylates giving the AuNPs a negative surface charge similar to that of the unconjugated citrate-capped AuNPs. Consequently, it is likely that antibodies experience similar interactions with unconjugated and DTSSP-modified AuNPs which have hydrolyzed. Therefore, it is reasonable that both methods, direct adsorption and DTSSP coupling chemistry, resulted in similar antibody surface coverages.

### **Conclusions**

We have developed a fluorescence-based method to directly quantify antibody adsorbed onto AuNPs. The method involves a three-step procedure, including dissolution of the AuNPs with KI/I<sub>2</sub>, isolation of adsorbed antibody via spin desalting columns, and protein quantification with NanoOrange, a fluorescent dye. Previous works to evaluate antibody adsorption onto AuNP are limited in that they indirectly infer the quantity of adsorbed antibody based on analysis of excess protein in solution or because they only provide a relative surface coverage. The novelty of this approach is that it directly analyses the antibodies adsorbed onto the AuNP and provides an absolute measurement of quantity.

To validate the method, we have quantified goat anti-mouse IgG antibody directly adsorbed onto AuNPs. We determined an absolute surface coverage of  $309 \pm 94$  antibodies per 60 nm AuNP. Moreover, we demonstrate that this novel method is more accurate than estimates

of absolute surface coverage based on mass difference between the added antibody and excess antibody remaining in solution after modification.

We anticipate that this method will be broadly applicable to enhancing applications utilizing protein-modified AuNP, and is not limited to antibody-modified AuNP. NanoOrange is sensitive to a range of targets, including large peptides, small proteins, and large proteins, such as IgG.<sup>56</sup> The most significant impact of this work, however, may be on the evaluation and comparison of novel conjugation chemistries aimed at protein orientation. It is well-accepted that the performance of technologies based on protein-modified nanoparticle is dependent upon both protein loading and protein orientation to maximize bioactivity. Therefore, it is necessary to quantify immobilized protein in any novel conjugation chemistry to ensure that enhanced performance is due to orientation rather than an increase in protein surface coverages.

## CHAPTER III

### CHEMICAL MODIFICATION OF ANTIBODY ENABLES PH INDEPENDENT FORMATION OF STABLE ANTIBODY-GOLD NANOPARTICLE CONJUGATES

#### **Introduction**

Protein modification of nanoparticles is essential to new and emerging biosensing technologies.<sup>1-3,69</sup> Antibody-gold nanoparticle conjugates are commonly used for novel biosensors due to their high specificity and broad applicability.<sup>70-72</sup> The sensitivity and stability of these biosensors is determined by the protein orientation and surface coverage on the gold nanoparticle, which are governed by the conjugation process of protein onto the gold nanoparticle surface.<sup>36,73,74</sup> An ideal immobilization method would ensure antibody conjugation and reliability for assay reproducibility and performance. This method would also need to ensure stabilization of the protein-nanoparticle conjugate in a variety of conditions without hindering assay performance. While there are several techniques to attach proteins onto gold nanoparticles, most simple techniques are dependent on the pH of the antibody.<sup>6,11,73,74</sup> This presents a challenge for the development of novel multiplexed assays in which multiple antibody-nanoparticle conjugates must be prepared and coexist in a single reagent suspension. Additional considerations include reversible immobilization and protein orientation on the surface of the gold nanoparticle.<sup>74-77</sup>

Immobilization of protein onto gold nanoparticles can occur through direct adsorption or use of a coupling agent for covalent attachment. Non-covalent direct adsorption is limited in that the attachment requires a unique and specific pH for each protein. It is well-established that for optimal adsorption the solution pH must be slightly higher than the isoelectric point (pI) of the protein.<sup>18,24,65</sup> Moreover, direct adsorption does not allow control over orientation of the



immobilized protein which can adversely affect protein biofunctionality, and it has been argued that non-covalent attachment allows for desorption which can result in short shelf-life and unwanted protein exchange.<sup>18,74</sup> However, it should be noted that we have not observed protein desorption or exchange from stable protein-gold nanoparticle conjugates that rely on direct adsorption for conjugate formation.<sup>78</sup>

To circumvent the concerns and challenges of direct adsorption, numerous approaches have been explored to immobilize protein onto gold nanoparticles through covalent coupling chemistry.<sup>79-84</sup> Carbohydrates if present on the protein can be used for attachment; however, along with being time intensive this method requires carbohydrates to be present on the protein and is labor intensive.<sup>19</sup>

Covalent modification of gold nanoparticles using bifunctional crosslinking chemistry molecules such as DTSSP (3,3'-dithiobis(sulfosuccinimidyl propionate)) is one of the most widely used method of attachment.<sup>13,85-94</sup> The attachment is said to occur by the sulfur binding to gold nanoparticles, leaving a terminal NHS (N-hydroxysuccinimide) ester group that attaches to the protein *via* the primary amine located on lysine.<sup>13,91,93</sup> This method however, requires the solution pH to be high enough for the lysine groups on the protein to be deprotonated; furthermore, it has been recently proposed that the hydrolysis of NHS occurs faster than aminolysis onto the primary amine.<sup>21,36</sup> This is because the reaction is limited to diffusion of the protein onto the NHS functionalized gold nanoparticle.<sup>21</sup> While there are several methods of attaching protein onto nanoparticles, the exact chemistry behind these methods is still relatively unknown, and there is also still a need for a fast universal method of attachment that is stable under a range of conditions.

In this chapter, we describe a novel approach to attach protein onto gold nanoparticles that is fast, is compatible with many antibodies, and generates stable conjugates for a wide range of pH values. To achieve this, we first modified the lysine residues on the protein with NHS-activated esters, DTSSP or NHS-acrylic acid, to alter the protein charge. The modified protein was then adsorbed onto the gold nanoparticles to form stable conjugates in high ionic strength suspensions independent of pH. We determined that this method can be utilized on a range of antibodies by forming stable conjugates with goat anti-mouse IgG, mouse anti-rabbit IgG, and rabbit anti-mouse IgG. Furthermore, we demonstrated that the modified antibody maintains bioactivity towards its target antigen in a functional assay.

## **Experimental**

### *Materials*

Gold nanoparticles (AuNPs; 60 nm) were purchased from Ted Pella Inc. (Redding, CA). Borate buffer, goat anti-mouse IgG polyclonal antibody, mouse anti-rabbit IgG polyclonal antibody, rabbit anti-mouse IgG polyclonal antibody, 3,3'-dithiobis[sulfosuccinimidylpropionate] (DTSSP), and Zeba spin desalting columns (7K MWCO, 0.5 mL) were acquired from Thermo Scientific (Rockford, IL). Acrylic acid N-hydroxysuccinimide ester (acrylic NHS), and Bovine serum albumin (BSA) were purchased from Sigma-Aldrich (St Louis, MO).  $K_2HPO_4$  was purchased from Mallinckrodt Chemical Inc. (Paris, KY).  $KH_2PO_4$  was purchased from Fisher Scientific (Waltham, MA). All aqueous solutions were prepared in NANOpure deionized water (18 M $\Omega$ ) from a Barnstead water purification system (Thermo Scientific, Rockford, IL).

### *Antibody-NHS Modification*

Five  $\mu\text{L}$  of NHS linker molecule (Acrylic acid NHS) or DTSSP at the desired concentration were added to 30  $\mu\text{g}$  of selected antibody and incubated for 2 hrs. Desalting columns were used to separate the excess linker molecule from the modified antibody. To empty the stacking buffer, the column was centrifuged at 3000g for 3 min, sample was loaded and 10  $\mu\text{L}$  of 2 mM borate buffer (pH 8.5) was added then the column was centrifuged at 3000g for 4 min. The modified antibody concentration was measured using a NanoDrop 2000c spectrophotometer (Thermo Scientific, Rockford, IL).

### *Protein Modified Gold Nanoparticles (pAuNPs)*

#### *Direct*

One hundred  $\mu\text{L}$  of 60 nm AuNPs were placed into a microcentrifuge tube, then 4  $\mu\text{L}$  of 50 mM phosphate buffer solution (pH 6.0, 6.5, 7.0, or 7.5) or 50 mM borate buffer (pH 8.0 or 8.5) were added to adjust the solution to the desired pH. Three  $\mu\text{g}$  of desired IgG protein (goat anti-mouse, mouse anti-rabbit, or rabbit anti-mouse) were then added to each solution and incubated for 20 min at room temperature. Next 10  $\mu\text{L}$  of 10 % (wt/v) NaCl were added and dynamic light scattering was used to evaluate the stability of the pAuNPs.

#### *DTSSP-Au*

One hundred  $\mu\text{L}$  of 60 nm AuNPs were placed into a microcentrifuge tube, then 4  $\mu\text{L}$  of 50 mM phosphate buffer solution (pH 6.0, 6.5, 7.0, or 7.5) or 50 mM borate buffer (pH 8.0 or 8.5) were added to adjust the solution to the chosen pH. One  $\mu\text{L}$  of 0.5 mM DTSSP was added and incubated for 1 hour at room temperature. The solution was then centrifuged at 5000g for 5

min, the pelleted AuNPs were resuspended in 100  $\mu$ L of 2 mM buffer solution at the desired pH. The centrifugation/resuspension processes were repeated twice to thoroughly remove excess unbound DTSSP. Three  $\mu$ g of IgG protein (goat anti-mouse, mouse anti-rabbit, or rabbit anti-mouse) were then added to the tube and incubated for 20 min, then 10  $\mu$ L of 10 % (wt/v) NaCl were added, and dynamic light scattering was used to check the stability.

#### *NHS-Antibody*

One hundred  $\mu$ L AuNPs were placed into a microcentrifuge tube, then 4  $\mu$ L of 50 mM phosphate buffer solution (pH 6.0, 6.5, 7.0, or 7.5) or 50 mM borate buffer (pH 8.0 or 8.5) were added to adjust the solution to the desired pH. Three  $\mu$ g of NHS modified IgG protein (goat anti-mouse, mouse anti-rabbit, or rabbit anti-mouse) were then added to each solution and incubated for 20 min at room temperature. Next, 10  $\mu$ L 10% (wt/v) NaCl were added and dynamic light scattering was used to check stability of the AuNPs.

#### *Protein Modified AuNP Immunoassay*

##### *Direct*

One hundred  $\mu$ L of 60 nm AuNPs were placed into a microcentrifuge tube, then 4  $\mu$ L of 50 mM borate buffer (pH 8.5) was added to adjust the solution to the desired pH. Three  $\mu$ g of goat anti-mouse IgG were inserted, and the solution was incubated overnight. Following incubation, the functionalized AuNPs were centrifuged at 5000g for 5 min, the supernatant was removed, and the pelleted nanoparticles were resuspended in 100  $\mu$ L of 2 mM borate buffer (pH 8.5). The centrifugation/resuspension processes were repeated twice to thoroughly remove excess unbound antibody. After the final centrifugation the pelleted nanoparticles were resuspended into 100  $\mu$ L of 1% (wt/v) BSA solution. Ten  $\mu$ L of 10% (wt/v) NaCl solution were

added to determine stability of the *p*AuNPs. Dynamic light scattering was collected to determine the hydrodynamic diameter of the modified nanoparticles.

#### *NHS-Antibody*

One hundred  $\mu\text{L}$  of 60nm AuNPs were placed into a microcentrifuge tube, then 4  $\mu\text{L}$  of 50 mM buffer solution (pH 6.0-8.5) was added to adjust the solution to the desired pH. Three  $\mu\text{g}$  of acrylic (NHS) modified goat anti-mouse IgG were added to the solution and incubated overnight. The solution was then centrifuged at 5000g for 5 min and resuspended in 100  $\mu\text{L}$  of 2 mM buffer solution at the desired pH. The centrifugation/resuspension process was repeated twice with the final resuspension being in 100  $\mu\text{L}$  of 1% (wt/v) BSA solution. Ten  $\mu\text{L}$  of 10% (wt/v) NaCl were added to check stability of the *p*AuNPs, and dynamic light scattering was collected to determine hydrodynamic diameter of the particles.

### **Instrumentation**

#### *Dynamic Light Scattering*

A BI-90Plus (Brookhaven Instruments Corporation, NY) armed with a 658 nm laser and an avalanche photodiode detector was used. The collection angle of the backscattered light was 90°. Each hydrodynamic diameter reported was the mean of three 30 s runs. The resultant data were analyzed using the MAS OPTION software.

#### *UV-Visible absorption*

A NanoDrop 2000c (Thermo Scientific, Rockford, IL), equipped with a xenon lamp was used for absorbance measurements. One  $\mu\text{L}$  of sample was added to the stage with an

illumination time of 5 s, the collection wavelength for quantification was set to 280 nm, and the concentration was calculated by the NanoDrop 2000/2000c software.

## **Results and Discussion**

### *Immobilization Methods*

Immobilization of antibodies onto the surface of gold nanoparticles is commonly performed via direct adsorption or NHS coupling chemistry. It is well established that antibodies directly adsorb onto gold nanoparticles (Figure 16A). While the mechanism is not fully understood, it is known that direct adsorption requires the pH to be slightly basic of the isoelectric point (pI) of the protein, and occurs through a combination of hydrophobic and electrostatic interactions.<sup>18,24</sup> To demonstrate this, goat anti-mouse IgG was incubated with 60 nm AuNPs in a pH range of 6.0-8.5 in increments of 0.5 pH units. At pH 6.0-7.5, the nanoparticles aggregated upon addition of the antibody within 5 min as indicated by a color change of the suspensions observed with the naked eye (Figure 17A).

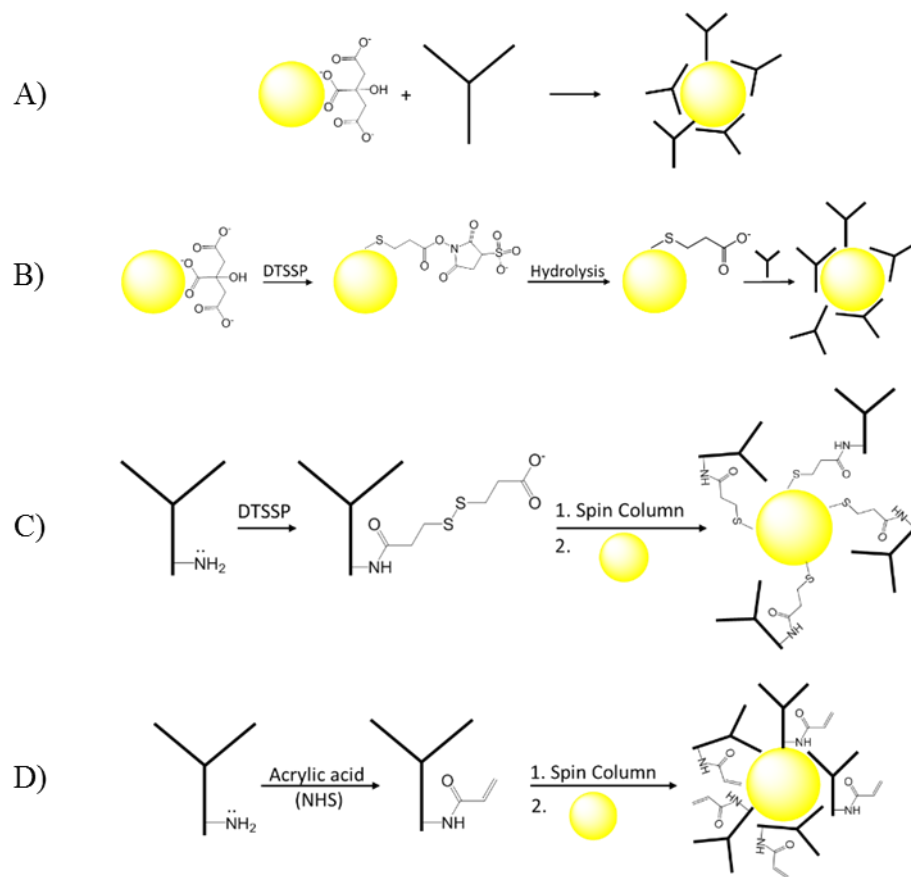


**Figure 16.** Schematic of the types of immobilization methods. A) Direct adsorption. B) DTSSP functionalized gold nanoparticles followed by antibody adsorption. C) DTSSP modified antibody followed by adsorption onto gold nanoparticles. D) Acrylic acid (NHS) modified antibody followed by adsorption onto gold nanoparticles.

This suggests that at the lower pH values, the protein was sufficiently protonated and carried sufficient positive charge that it caused the gold nanoparticles to aggregate rather than form a stable protein-gold nanoparticle conjugate. At  $\text{pH} \geq 8.0$ , the AuNP remained red after the addition of antibody; however, this does not confirm that antibody adsorbed onto the AuNP.

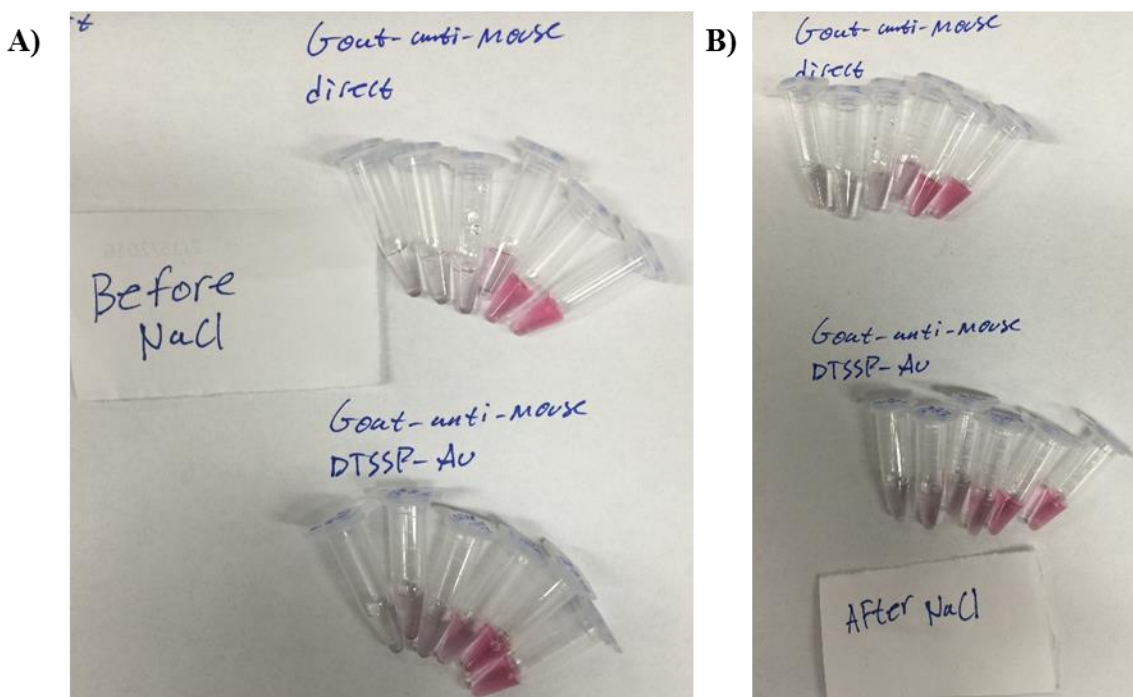


**Figure 17.** Goat anti-mouse IgG functionalized gold nanoparticles by direct adsorption and by DTSSP functionalized gold nanoparticles before the addition of antibody. Both at a pH range of 6.0-8.5 from left to right. A) Before the addition of NaCl. B) After the addition of NaCl to a final concentration of 1 % (wt/v).

A coagulation test was used to assess adsorption of antibody onto the AuNP to form a stable conjugate.<sup>24</sup> Sodium chloride was added to the antibody-AuNP suspension and dynamic light scattering (DLS) was used to measure the hydrodynamic diameter ( $D_H$ ) of the modified AuNPs. A stable conjugate has a  $D_H$  of ~85-90 nm, consistent with the size of an IgG adlayer, while unconjugated AuNP will undergo aggregation to form larger assemblies in the presence of electrolyte.<sup>6</sup> Direct adsorption of antibody onto AuNP at pH 8.0 and 8.5 form conjugates with a  $D_H$  of 86.9 nm and 89.2 nm after the addition of NaCl, respectively, and are consistent with other



reported data for stable AuNP-antibody conjugates (Figure 18, Table 1). Goat anti-mouse IgG has a pI range of 6.5-9.5,<sup>95</sup> thus, these data are consistent with other works demonstrating that the pI or charge of the protein plays a direct role in the adsorption of protein onto gold nanoparticles.

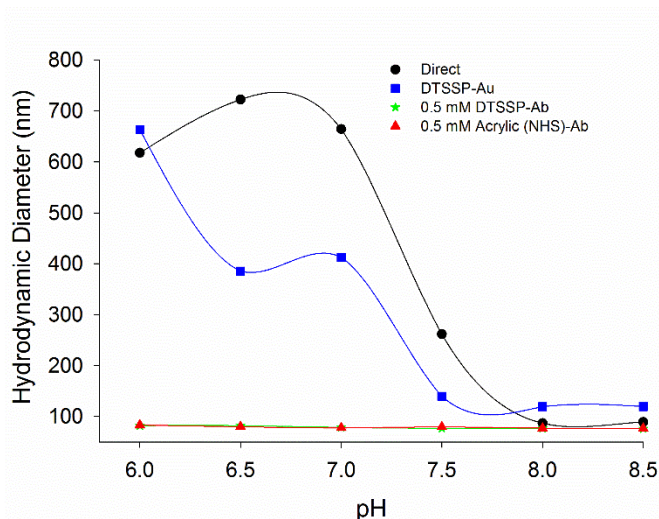


**Figure 18.** DLS of antibody functionalized gold nanoparticles after the addition of NaCl. Goat anti-mouse IgG immobilized using direct adsorption, DTSSP functionalized AuNPs, DTSSP modified antibody, or acrylic acid (NHS) modified antibody.

It has long been suggested that covalent coupling of antibody to AuNP with heterobifunctional cross-linker such as 3,3'-dithiobis(sulfosuccinimidyl propionate) (DTSSP) results in a more stable and robust conjugation that prevents desorption (Figure 16B).<sup>13</sup> This chemistry requires basic conditions to deprotonate lysine residues thereby enabling aminolysis. A recent study demonstrated that hydrolysis of DTSSP on the AuNP surface occurs faster than aminolysis.<sup>21</sup> Thus, the DTSSP-modified AuNP hydrolyzes to present a terminal carboxylate on the surface of the AuNP, yielding a similar surface charge as the original citrate capped AuNP. If

this is the case, immobilization of the antibody to DTSSP-modified AuNP should be similar to direct adsorption to citrate-capped AuNP and show the same pH dependence. To this end, DTSSP was attached to AuNPs prepared in buffers ranging from pH 6.0-8.5, excess DTSSP was removed *via* centrifugation of the DTSSP-AuNP conjugates, and goat anti-mouse IgG was added to each solution. At pH 6.0-7.5, the nanoparticles aggregated upon addition of the antibody within 5 min as indicated by a color change of the suspensions observed with the naked eye (Figure S4A). At pH  $\geq$  8.0, the AuNP remained red after the addition of antibody, and a salt-induced coagulation test was performed to confirm immobilization of the antibody onto the AuNP. DLS measured a  $D_H$  of 119.3 nm and 119.6 nm at pH 8.0 and 8.5, respectively, indicating the formation of moderately stable conjugates. Collectively, similar pH dependent trends were observed for the immobilization of antibody onto citrate-capped and DTSSP-modified AuNP. These results suggest that the DTSSP adlayer hydrolyzed and the antibody is not covalently attached to the AuNP through DTSSP to form a conjugate, rather the antibody attached through a direct adsorption mechanism similar to that of the citrate capped AuNP.

**Table 1.** Stability of goat anti-mouse IgG in 1 % (wt/v) NaCl solution using the varying conjugation techniques over a pH range of 6-8.5. pH vs hydrodynamic diameter measured with DLS.

pH	Direct	DTSSP-Au	Hydrodynamic Diameter (nm)			0.5 mM Acrylic acid (NHS)	5 mM Acrylic acid (NHS)
			0.5 mM DTSSP	1 mM DTSSP	5 mM DTSSP		
6	617.9	663.7	82	79.5	153.8	83.2	74.9
6.5	722.5	385.7	82	79	190.4	79.8	75.9
7	664.5	412.9	78.6	78.1	254.6	77.8	73.5
7.5	261.6	139.5	76.9	78.1	226.6	79.4	69.1
8	86.9	119.3	76.7	77.6	597.2	77.2	71.4
8.5	89.2	119.6	76.2	78.1	681.3	76.6	71.6

We hypothesized that addition of free DTSSP, i.e., not assembled on AuNP, directly to antibody would result in chemical coupling between the DTSSP and antibody. Free DTSSP is not limited to the surface of the AuNP and can be prepared at a higher concentration to drive aminolysis rather than hydrolysis of the DTSSP. The DTSSP modified antibody can then chemisorb onto the AuNP in a second step via self-assembly through the disulfide moiety to form a robust conjugate. Moreover, the DTSSP modification would eliminate the positive charge of protonated lysine that is responsible for AuNP aggregation at pH values of 6.0-7.5 as demonstrated above. To test this hypothesis, 0.5 mM DTSSP was incubated with goat anti-mouse IgG, and the excess DTSSP was removed *via* size exclusion desalting column. (Figure 16C) The purified DTSSP-antibody conjugate was then added to 60 nm gold nanoparticles at various pH values (6.0-8.5). Notably, no visual aggregation was observed upon addition to the AuNP at any pH; this is in contrast to the aggregation induced by the addition of unmodified antibody to AuNP at low pH values detailed above (Figure 19A). This observation is strong evidence that DTSSP reacted with the antibody to alter its interaction with AuNP.

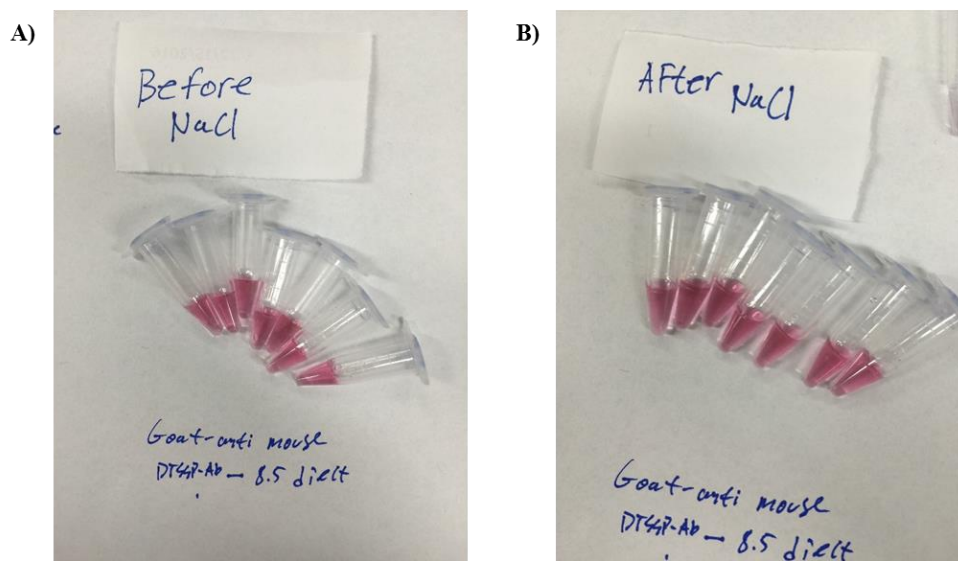


**Figure 19.** Goat anti-mouse IgG modified with 0.5 mM DTSSP conjugated onto 60 nm gold nanoparticles. Conjugated at pH values 6.0-8.5 from left to right followed by direct adsorption at pH 8.5. A) Before the addition of NaCl. B) After the addition of NaCl to a final concentration of 1 % (wt/v).

A coagulation test was conducted to assess immobilization of the DTSSP-modified antibody onto the AuNP to form a stable conjugate. Upon addition of NaCl to each suspension the hydrodynamic diameter was measured *via* DLS and ranged between 76.2 nm to 82.0 nm for the entire pH range (Figure 18, Table 1). These data confirm that DTSSP chemically modified the antibody and the modified antibody is immobilized onto the AuNP, independent of pH, to form a stable conjugate. Furthermore, it was inferred that the adsorption process of the DTSSP modified protein onto gold nanoparticles was driven by the disulfide functionality imparted by the DTSSP.

### *Acrylic Acid (NHS)*

In order to confirm that the sulfur from DTSSP was in fact driving the adsorption process onto gold nanoparticles as hypothesized, the antibody was modified with NHS-acrylic acid rather than DTSSP. Similar to DTSSP, the NHS-acrylic acid couples to the antibody by means of the *N*-hydroxysuccinimidyl ester group *via* aminolysis with lysine; however, unlike DTSSP, the acrylic acid does not provide any linking chemistry such as a disulfide for chemisorption to the AuNP. Therefore, it was anticipated that the formation of a stable conjugate with the NHS acrylic modified antibody would result from direct adsorption and demonstrate a pH dependence. To confirm this hypothesis, 0.5 mM acrylic acid (NHS) was incubated with goat anti-mouse IgG and the excess NHS acrylic acid was removed *via* size exclusion desalting column. The purified acrylic acid modified antibody was then added to 60 nm gold nanoparticles at various pH values (6.0-8.5) (Figure 16D). The AuNP remained stable upon addition of the modified antibody at all pH values tested, similar to the DTSSP modified antibody (Figure 20A), confirming that the lysine had been neutralized by the NHS-acrylic acid.

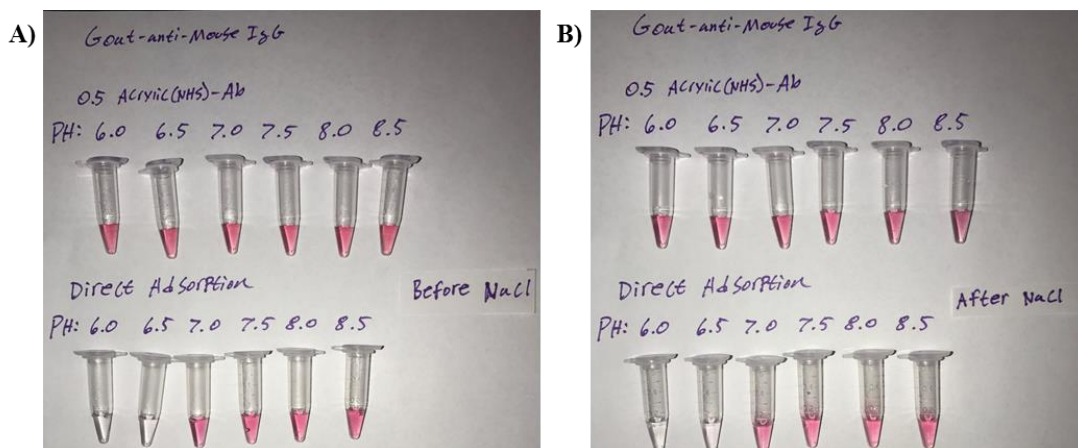


**Figure 20.** Goat anti-mouse IgG modified with 0.5 mM acrylic (NHS) (top) and by direct adsorption (bottom) conjugated onto 60 nm gold nanoparticles. Conjugated at pH values 6.0-8.5 from left to right. A) Before the addition of NaCl. B) After the addition of NaCl to a final concentration of 1 % (wt/v).

A salt-induced coagulation test was performed to evaluate the stability of the conjugates using DLS to measure the  $D_H$  (Figure 18, Table 1). Interestingly, the measured  $D_H$  was between 76.6 nm and 83.2 nm, indicating the formation of stable conjugates at all pH values (6.0-8.5). These results contradict our hypothesis that the disulfide of DTSSP was responsible for forming stable conjugates at  $6.0 \leq \text{pH} \leq 7.5$ . The stability of these conjugates reveals that the NHS acrylic acid modified antibody must be adsorbing onto AuNPs *via* direct adsorption, e.g., hydrophilic, hydrophobic, electrostatic, and native thiols of the cysteine residues. Moreover, these antibody modifications indicate that antibodies can be immobilized onto AuNP over a wide range of pH values without bifunctional coupling agents provided that the basic lysine residues are converted to a chemical moiety such that the charge is no longer pH dependent.

To establish broad applicability of this conjugation method, AuNP conjugates were synthesized with mouse anti-rabbit IgG (mIgG) or rabbit anti-mouse IgG (rIgG). For each antibody, conjugates were prepared using unmodified, DTSSP modified, and acrylic acid modified antibody at pH values ranging from 6.0 to 8.5. The AuNP were stable after the addition of unmodified, DTSSP modified, and acrylic acid modified mouse anti-rabbit IgG at all pH values. Surprisingly, all the prepared mouse anti-rabbit IgG conjugates (unmodified and modified) were stable upon addition of NaCl at each pH, with a  $D_H$  ranging from 73 – 95 nm (Figure 21, Table 2). The stability of the conjugates prepared with unmodified antibody over the pH range shows that mouse anti-rabbit IgG is less pH dependent than other proteins tested.

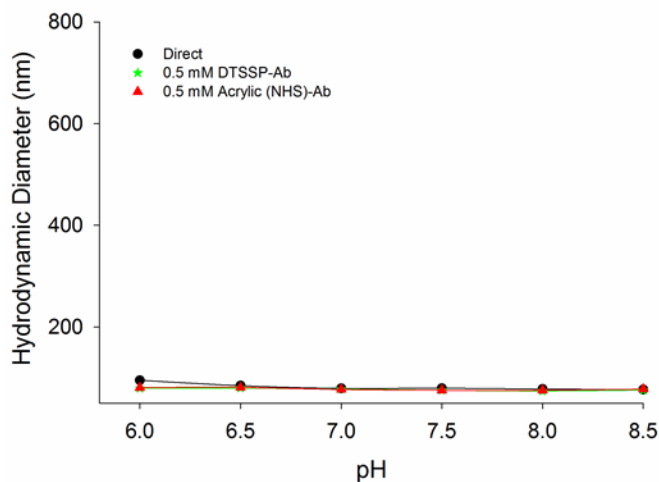


**Figure 21.** DLS of mouse anti-rabbit IgG functionalized gold nanoparticles after the addition of NaCl. Mouse anti-rabbit IgG immobilized using direct adsorption, DTSSP modified antibody, and acrylic acid (NHS) modified antibody.

**Table 2.** Stability of mouse anti-rabbit IgG in 1 % (wt/v) NaCl solution using the varying conjugation techniques at a pH range of 6-8.5. pH vs hydrodynamic diameter measured with DLS.

pH	Direct	Hydrodynamic Diameter (nm)			0.5 mM Acrylic acid (NHS)	5 mM Acrylic acid (NHS)
		0.5 mM DTSSP	1 mM DTSSP	5 mM DTSSP		
6	95	79.3	80.3	151.9	80.3	229.9
6.5	84.3	79.6	79	144.4	80.8	227
7	79.1	77.6	80.2	153.3	76.9	303.8
7.5	79.3	75.4	80.8	281.3	75.3	256
8	77.7	73.9	113.4	436.5	75.3	223.1
8.5	76.7	75.7	120.7	525	77.5	357.5

Conversely, the unmodified rIgG immediately caused the AuNPs to aggregate at all pH values prior to the addition of NaCl. Addition of the DTSSP and acrylic acid modified rabbit anti-mouse IgG did not cause the AuNP to aggregate; however only the DTSSP modified rabbit anti-mouse IgG at pH 8.0 and 8.5 resulted in a stable conjugate to resist salt induced aggregation (Figure 22, Table 3).

To further investigate this modification effect, rabbit anti-mouse IgG was modified with NHS (0.5 mM DTSSP and 0.5 mM acrylic acid (NHS)), and unmodified in the same pH range (6.0-8.5). Upon the addition of NaCl, DLS was measured and the hydrodynamic diameter for all samples was well over 100 nm showing aggregation for the modified protein-AuNP conjugates, and unmodified protein-AuNP conjugates. (Table 3) In an effort to stabilize rabbit anti-mouse IgG conjugated onto gold nanoparticle, the NHS concentration was varied: 1 mM DTSSP, and 5 mM DTSSP were used in the modification procedure. Upon the addition of NaCl and DLS measurement, the 1 mM DTSSP aggregated, while 5 mM DTSSP modified rabbit anti-mouse



IgG was stable in the entire pH range (6.0-8.5) (Figure 22, Table 3). This led us to test the acrylic acid (NHS) modification at a 5 mM concentration as well (Figure 22). Table 3 shows that the hydrodynamic diameter for these was also over 100 nm for each sample.

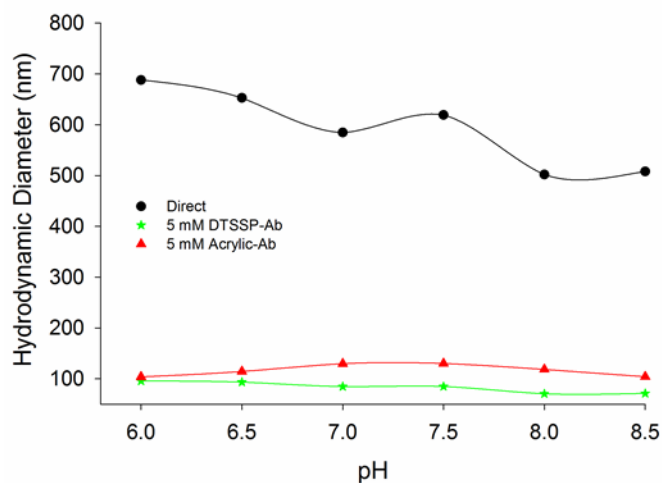


**Figure 22.** DLS of rabbit anti-mouse IgG functionalized gold nanoparticles after the addition of NaCl. Rabbit anti-mouse IgG immobilized using direct adsorption, DTSSP modified antibody, and acrylic acid (NHS) modified antibody.

**Table 3.** Stability of rabbit anti-mouse IgG in 1 % (wt/v) NaCl solution using the varying conjugation techniques at a pH range of 6-8.5. pH vs hydrodynamic diameter measured with DLS.

pH	Direct	Hydrodynamic Diameter (nm)			0.5 mM Acrylic acid (NHS)	5 mM Acrylic acid (NHS)
		0.5 mM DTSSP	1 mM DTSSP	5 mM DTSSP		
6	688.1	510.2	266.9	95.5	352.9	103.8
6.5	652.8	486.8	274.1	93.4	398.1	114.4
7	584.7	478.1	261.3	84.6	421.4	129.7
7.5	619.3	447.1	223.7	84.8	427.6	130.1
8	502	457	204.7	70.5	454.3	118.4
8.5	508.1	439.8	160.8	71.2	433.2	104.1

Because it is known that the pI of an antibody is where it has a net neutral charge, and that the pH for optimal binding *via* direct adsorption is slightly higher than the pI of the antibody. We hypothesize that this stabilization at 5 mM DTSSP but instability at 5 mM acrylic acid is due to the charge on the protein. While both DTSSP and acrylic acid (NHS) react with lysine groups, DTSSP is changing the charge on the lysine from positive to negative, while acrylic acid (NHS) is changing it from a positive charge to neutral. The instability at the lower concentrations of NHS (0.5 mM) suggest that the antibody has not been neutralized enough for optimal binding onto gold nanoparticles.

This motivated us to test multiple concentrations of DTSSP, and acrylic acid (NHS) for each antibody used to test our hypothesis. Table 1 shows our full analysis of goat anti-mouse IgG with multiple concentrations of DTSSP and acrylic acid (NHS). At a concentration of 5 mM, the DTSSP modification aggregated (well over 100 nm) at all pH values in the 6.0-8.5 range when introduced to a 1% (wt/v) NaCl solution, however the 5 mM acrylic acid (NHS) was stable

(between 75 nm and 85 nm) at all pH values in the same environment (Table 1). Upon performing the same experiment with mouse anti-rabbit IgG, both 5 mM DTSSP and 5 mM acrylic acid (NHS) modification were aggregated (well over 100 nm) in the entire pH range (6.0-8.5) (Table 2). With rabbit anti-mouse IgG (Table 3) stability is only fully effective at a 5 mM concentration of DTSSP. When using 5 mM acrylic acid (NHS), the aggregates measured with DLS are smaller than that obtained from direct adsorption, but are not completely stable. All antibodies differ in the amount of lysine groups present, therefore it would be reasonable to assume that each would require a unique concentration of the NHS modification. When modifying an antibody with acrylic acid (NHS) the lysine group changes from a positive terminus, to a neutral charge; however, when modifying with DTSSP, it changes from the positive to a negative form. Because the stability of the AuNP-antibody conjugates does not depend on the sulfur group from DTSSP, the stability of these conjugates must be related to the charge on the surface of the antibody. Since all antibodies differ in the amount of lysine, it would make sense that each would require a unique concentration of the NHS modification.

#### *Amino Acid Analysis*

To further investigate this hypothesis, amino acid analysis was performed on each of the antibodies used in the experiment. The lysine:IgG ratio was different for each protein studied. Goat anti-mouse IgG had a ratio of 4.98, while mouse anti-rabbit had a ratio of 4.23, and rabbit anti-mouse had a ratio of 20.10. These ratios align with the concentration of NHS modification needed to stabilize the proteins onto AuNPs. Goat anti-mouse IgG (Table 1) having a lysine:IgG ratio of 4.98, only needed 0.5 mM NHS modification to neutralize the charge. Mouse anti-rabbit IgG (Table 2) lysine:IgG ratio of 4.23 was stable without modification of NHS and at 0.5 mM NHS modification. Both the goat (Table 1) and mouse (Table 2) antibodies were not stable at a

higher concentration of NHS (5.0 mM), this suggest that modifying all the lysine groups has an adverse effect to the binding ability onto a gold nanoparticle. Rabbit anti-mouse IgG (Table 3) has a larger lysine:IgG ratio of 20.10 causing it only to be stable when the lysine is changed to a negative charge with DTSSP at a concentration of 5 mM.

### *Modified Antibody Functionality*

It is reasonable to assume that there are lysine groups on both the Fc and Fab regions of the IgG molecule; thus, modifying lysine on the Fab region could induce an adverse effect on binding to the antigen. To determine the viability of the antibody-antigen binding after NHS modification, we performed an aggregation based assay utilizing DLS.<sup>6</sup> Goat anti-mouse IgG was modified with acrylic acid (NHS), then incubated with 60 nm AuNPs over a pH range of 6.0-8.5. This was compared to a direct adsorption assay with goat anti-mouse IgG on 60 nm AuNPs at pH 8.5. A typical DLS assay is performed with direct adsorption at pH 8.5, consequently direct adsorption at pH 8.5 was used to compare to the acrylic acid (NHS) modified antibody at pH 6.0- 8.5 at a sample concentration range of 0.5 ng/mL to 5000 ng/mL. Acrylic acid (NHS) was used instead of DTSSP for two reasons; it is cheaper, and it should not bind to AuNPs when free in solution like DTSSP; it is possible that the spin column step could be removed making it faster and cheaper. The modification of the antibody lysine groups with NHS did not stop the aggregation assay from performing as expected at the entire pH range (Figure 23, Table 2), confirming that the antibody modification does not hinder the antibody-antigen binding.

**Table 4.** Hydrodynamic diameter ( $D_H$ ) increase of the DLS assay with acrylic acid (NHS) modified goat anti-mouse IgG at a pH range of 6.0-8.5, and direct adsorption at pH 8.5

**Average Hydrodynamic Diameter Increase (nm)**

Conc (ng/mL)	Acrylic acid (NHS)						Direct
	pH 6.0	pH 6.5	pH 7.0	pH 7.5	pH 8.0	pH 8.5	pH 8.5
5000	18.7	14.4	12.8	13.5	11.6	11.3	18.2
500	44.7	44.3	47.1	37.9	46.8	38.1	80.0
50	97.3	94.9	83.4	81.1	71.9	64.4	143.4
5	35.9	33.4	19.7	19.2	14.9	12.5	35.7
0.5	5.9	4.5	3.8	2.3	0.5	2.2	3.2
PBS	0.0	0.0	0.0	0.0	0.0	0.0	0.0

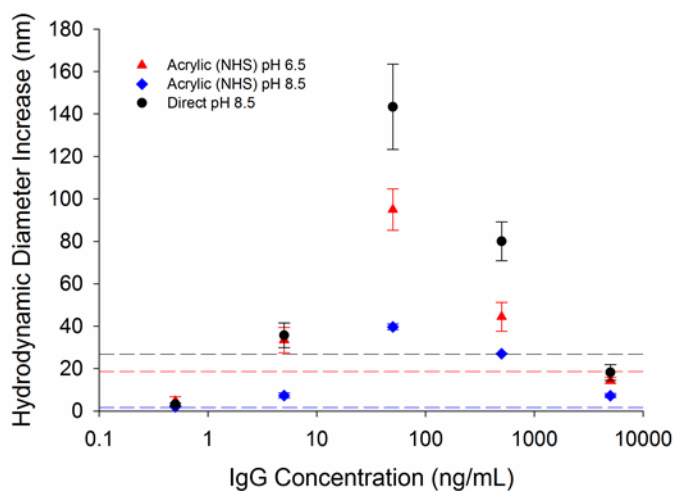


**Figure 23.** Calibration curve of the DLS immunoassay with goat anti-mouse IgG showing the  $D_H$  increase with respect to concentration of IgG. Direct adsorption at pH 8.5 and acrylic acid (NHS) modified at pH 6.5 and 8.5, as shown the error bars represent the standard deviation of 3 independent assays. The dashed lines represent the limit of detection for each immobilization method.

The data in Figure 23 and Table 4 show that when the acrylic acid (NHS) assay is performed at a lower pH it has larger aggregation. While pH 6.0 had the largest hydrodynamic diameter increase, pH 6.5 was used because it is close to physiological pH in addition to having large aggregation. Figure 23 illustrates the hooking effect in the extended calibration curve of the assay, we wanted to zoom onto the linear range of the assay to compare analytical figures of merit of the new assay to those of direct adsorption. Figure 24A shows the assay of direct adsorption and acrylic acid (NHS) modified antibody from 0.1 ng/mL to 50 ng/mL. This assay also reached a maximum at 10 ng/mL for direct adsorption and 25 ng/mL for acrylic acid (NHS) modified.

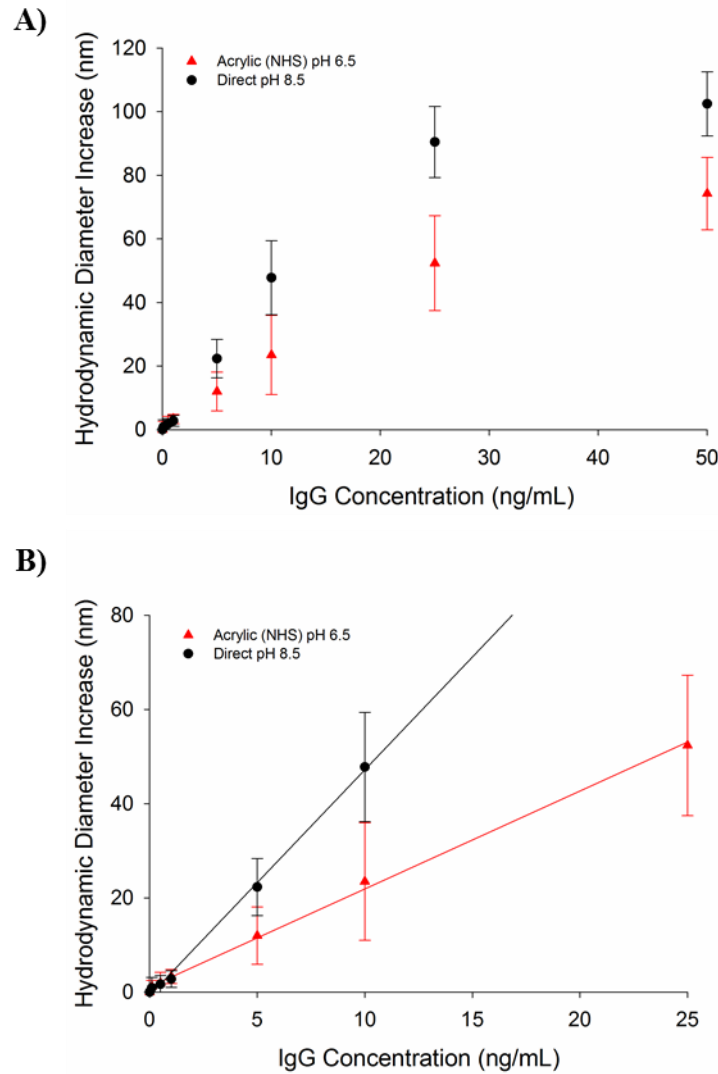


**Figure 24.** Calibration curve of goat anti-mouse IgG with direct adsorption at pH 8.5 and acrylic acid modified at pH 6.5. A) Lower range of the calibration curve, error bars are the standard deviation of 3 independent assays. B) Trendline of the linear portion of the graph.

The linear portions of each calibration curve were used for linear regression and analytical figures of merit (Figure 24B). The acrylic acid (NHS) modified antibody DLS assay at pH 6.5 behaved similar to the direct adsorption DLS assay. Table 5 list the analytical figures of

merit for each assay demonstrating that the assay is not only viable, but its performance is comparable to the direct adsorption assay.

**Table 5.** Figures of merit for the dynamic light scattering immunoassay with goat anti-mouse IgG comparing direct adsorption at pH 8.5 to acrylic acid (NHS) modified antibody at pH 6.5.

<b>Figures of Merit for Goat Anti-Mouse IgG</b>		
	<b>Direct pH 8.5</b>	<b>Acrylic (NHS) pH 6.5</b>
<b>Min. det. Signal (nm)</b>	2.16	1.90
<b>LOD (ng/mL)</b>	0.59	0.38

Once the best pH was determined, we wanted to explore the above hypothesis of modifying antibody with acrylic acid (NHS) and not using a spin column to remove the free acrylic acid (NHS). To this end goat anti-mouse IgG was incubated with acrylic acid (NHS), then added to gold nanoparticles without using a spin column to remove the excess acrylic acid (NHS). Acrylic acid (NHS) modified goat anti-mouse IgG with excess NHS removed *via* spin column was performed alongside to control the experiment. As shown in Figure 25, the spin column is not needed for the assay to function properly and the values are well within error even when compared to the data in table 4.



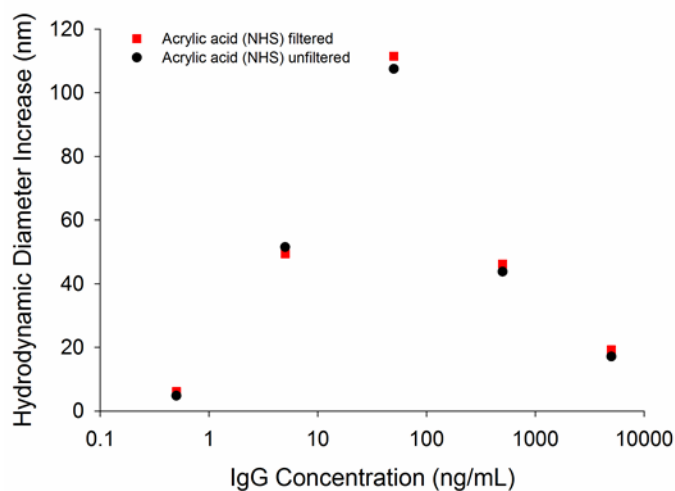


**Figure 25.** Calibration curve of acrylic acid (NHS) modified goat anti-mouse IgG at pH 6.5 with and without filtering *via* a spin column.

### Conclusions

We have established that the modification of antibody with bifunctional crosslinking molecules reduces the overall positive charge of the antibody allowing for direct adsorption onto gold nanoparticles and stabilization over a range of pH values. We show this method is effective on multiple antibodies demonstrating broad applicability, which has implications for a broad impact on novel immunoassay development. When compared, unmodified *vs* modified antibody with our dynamic light scattering immunoassay both detection limits were essentially identical ~1.0 ng/mL. This concludes that modification has not affected the active site of the antibody.

## CHAPTER IV

### CONCLUSIONS AND FUTURE DIRECTIONS

#### **Research Summary**

The results from this investigation lead to several new insights on protein modified gold nanoparticle immunoassays. The first part of the work focused on the development of a novel fluorescence based detection method for the direct quantification of antibody immobilized onto gold nanoparticles. This method focused on dissolving the gold nanoparticle using a KI/I<sub>2</sub> etchant solution with the proteins adsorbed onto the surface of the nanoparticle. The gold ions were filtered out using a size exclusion spin column to obtain the purified antibody. The isolated antibody was then tagged with NanoOrange a fluorescent dye that is capable of detecting low concentrations of protein. From this assay we determined  $309 \pm 93$  antibodies adsorb onto a 60 nm gold nanoparticles which is consistent with a fully adsorbed monolayer based on the footprint of an IgG molecule. We confirmed that multilayers do not form on the surface of a gold nanoparticle by measuring a hydrodynamic diameter increase from 62 nm unconjugated to 76 nm conjugated. Finally we used a more conventional method of antibody quantification by supernatant analysis which overestimated the surface coverage at  $660 \pm 87$  antibodies per nanoparticle demonstrating that our fluorescence based method is a more accurate substitute to the typical approach.

This fluorescence assay is not only able to detect large proteins such as IgG but also small proteins and large peptides. Perhaps the most impact this work will have is on the comparison of new conjugations chemistries towards protein orientations. The performance of protein modified nanoparticle based sensors is dependent on the number of immobilized proteins and the orientation to exploit the bioactivity of the protein. Thus, quantification of immobilized protein is imperative to the performance of new and emerging immobilization techniques based

on orientation to confirm that higher performance is from orientation not an increase in protein on the nanoparticle surface.

The second part of this work was to find an immobilization method for antibody onto gold nanoparticles that is independent of pH. Conventional methods such as direct adsorption or bifunctional crosslinking chemistry rely on isoelectric point of the antibody of choice. This is limiting when working with multiple antibodies in the same solution conditions that are needed for novel gold nanoparticle based immunoassays capable of multiplex detection. To achieve stable antibody-gold nanoparticle conjugates independent of pH we first modified the antibody with DTSSP or acrylic acid (NHS); these molecules are known to form an amide bond between the carboxyl group from the molecules and at terminal amine from lysine. We tested this method *via* a coagulation test and performed dynamic light scattering to ensure stable conjugates. We show broad applicability of the method by testing it with three different antibodies: goat anti-mouse IgG, rabbit anti-mouse IgG, and mouse anti-rabbit IgG. We found that by modifying the antibody with DTSSP the positively charged lysine is converted to a negative charge from the terminal carboxyl upon hydrolysis of the DTSSP molecule after modification. Similarly, when using acrylic acid (NHS) the lysine transformed from positive to neutral. This has significance because adsorption of the antibody to gold nanoparticles is based on the isoelectric point of the antibody and by changing the isoelectric point we can effectively manipulate the antibody to stabilize under conditions it previously had not been stable. Finally, to ensure the antibody modification was not hindering the active site of the antibody a dynamic light scattering immunoassay was performed against the conventional direct adsorption method and it was found that the detection limit of both assays was ~1.0 ng/mL. This work significantly enhances the field by providing a novel method of immobilization that is independent of pH. For the

achievement of multiplex detection of protein based nanosensors, these sensors must have protein immobilized and stable under the same solution conditions.

### **Outlook and Future Directions**

In the field of nanoscience there are many protein modified gold nanoparticle assays and sensors. This work provides insights on the protein-gold nanoparticle interface which could be utilized for many novel nanoparticle based sensors. These nanosensors are important for new rapid screening techniques utilizing methods such as surface enhanced Raman spectroscopy (SERS). SERS has low detection limits and multiplexing capabilities which is something the Driskell lab is working toward. This work has applications in comparing the activity of an antibody on a surface to the number of antibodies immobilized for determining the number of active antibodies immobilized on the surface *vs* inactive, something that should be considered when developing a new detection method using nanosensors.

Future directions of this work would be the utilization of the immobilization method in new gold nanoparticle based immunoassays developed in the Driskell lab. A direction the lab is currently focusing is the use of Fab portions of the antibody. Immobilization with the Fab portions could lead to a higher density of active sites on the surface of the nanoparticle thus, an improved assay. Previously our lab used goat anti-mouse Fab fragments and was unable to form stable Fab-AuNP conjugates. While a 60 nm gold nanoparticle with Fab conjugated onto it should have a hydrodynamic diameter ( $D_H$ ) around 65-75 nm in a 1 % (wt/v) NaCl solution, previous efforts using direct adsorption were only able to obtain 147.9 nm  $D_H$  indicating aggregation of the Fab-nanoparticle conjugates. Using acrylic acid (NHS) we were able to obtain stable conjugates with  $D_H$  from 66.2 nm to 73.2 nm. We performed an assay with the acrylic Fab

and compared it with our whole acrylic acid (NHS) modified goat anti-mouse IgG assay as shown in Figure 26.

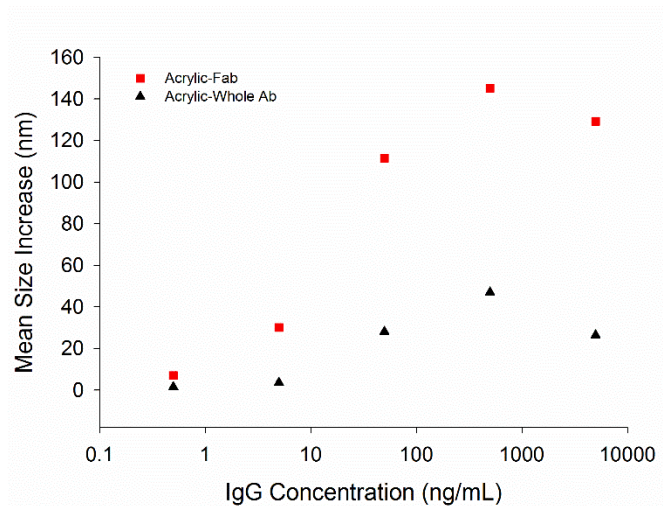


**Figure 26.** DLS with mean  $D_H$  increase vs IgG concentration comparing whole antibody vs Fab fragment.

The Fab assay proved to have a much greater sensitivity than the whole antibody. This is promising evidence that this assay could lead to lower limits of detection and perform faster than previous assays we have developed. We could also co-functionalize the acrylic-Fab antibody onto AuNPs and possibly perform a solution SERS assay, something that has been a goal of the Driskell lab group.

## REFERENCES

- (1) Jans, H.; Huo, Q. Gold Nanoparticle-Enabled Biological and Chemical Detection and Analysis. *Chemical Society Reviews* **2012**, *41*, 2849-2866.
- (2) Li, Y.; Schluesener, H. J.; Xu, S. Gold Nanoparticle-Based Biosensors. *Gold Bulletin* **2010**, *43*, 29-41.
- (3) Zhou, W.; Gao, X.; Liu, D.; Chen, X. Gold Nanoparticles for in Vitro Diagnostics. *Chemical Reviews* **2015**, *115*, 10575-10636.
- (4) Endo, T.; Kerman, K.; Nagatani, N.; Hiepa, H. M.; Kim, D.-K.; Yonezawa, Y.; Nakano, K.; Tamiya, E. Multiple Label-Free Detection of Antigen–Antibody Reaction Using Localized Surface Plasmon Resonance-Based Core–Shell Structured Nanoparticle Layer Nanochip. *Analytical Chemistry* **2006**, *78*, 6465-6475.
- (5) Elghanian, R.; Storhoff, J. J.; Mucic, R. C.; Letsinger, R. L.; Mirkin, C. A. Selective Colorimetric Detection of Polynucleotides Based on the Distance-Dependent Optical Properties of Gold Nanoparticles. *Science* **1997**, *277*, 1078-1081.
- (6) Lai, Y. H.; Koo, S.; Oh, S. H.; Driskell, E. A.; Driskell, J. D. Rapid Screening of Antibody–Antigen Binding Using Dynamic Light Scattering (DLS) and Gold Nanoparticles. *Analytical Methods* **2015**, *7*, 7249-7255.
- (7) James, A. E.; Driskell, J. D. Monitoring Gold Nanoparticle Conjugation and Analysis of Biomolecular Binding with Nanoparticle Tracking Analysis (NTA) and Dynamic Light Scattering (DLS). *Analyst* **2013**, *138*, 1212-1218.

- (8) Driskell, J. D.; Jones, C. A.; Tompkins, S. M.; Tripp, R. A. One-Step Assay for Detecting Influenza Virus Using Dynamic Light Scattering and Gold Nanoparticles. *Analyst* **2011**, *136*, 3083-3090.
- (9) Liu, X.; Dai, Q.; Austin, L.; Coutts, J.; Knowles, G.; Zou, J.; Chen, H.; Huo, Q. A One-Step Homogeneous Immunoassay for Cancer Biomarker Detection Using Gold Nanoparticle Probes Coupled with Dynamic Light Scattering. *Journal of the American Chemical Society* **2008**, *130*, 2780-2782.
- (10) Jeanmaire, D. L.; Van Duyne, R. P. Surface Raman Spectroelectrochemistry: Part I. Heterocyclic, Aromatic, and Aliphatic Amines Adsorbed on the Anodized Silver Electrode. *Journal of Electroanalytical Chemistry and Interfacial Electrochemistry* **1977**, *84*, 1-20.
- (11) Lopez, A.; Lovato, F.; Oh, S. H.; Lai, Y. H.; Filbrun, S.; Driskell, E. A.; Driskell, J. D. Sers Immunoassay Based on the Capture and Concentration of Antigen-Assembled Gold Nanoparticles. *Talanta* **2016**, *146*, 388-393.
- (12) Wang, G.; Park, H.-Y.; Lipert, R. J.; Porter, M. D. Mixed Monolayers on Gold Nanoparticle Labels for Multiplexed Surface-Enhanced Raman Scattering Based Immunoassays. *Analytical Chemistry* **2009**, *81*, 9643-9650.
- (13) Grubisha, D. S.; Lipert, R. J.; Park, H.-Y.; Driskell, J.; Porter, M. D. Femtomolar Detection of Prostate-Specific Antigen: An Immunoassay Based on Surface-Enhanced Raman Scattering and Immunogold Labels. *Analytical Chemistry* **2003**, *75*, 5936-5943.
- (14) Schroeder, H. W.; Cavacini, L. Structure and Function of Immunoglobulins. *The Journal of Allergy and Clinical Immunology* **2010**, *125*, S41-S52.
- (15) Kallewaard, Nicole L.; Corti, D.; Collins, Patrick J.; Neu, U.; McAuliffe, Josephine M.; Benjamin, E.; Wachter-Rosati, L.; Palmer-Hill, Frances J.; Yuan, Andy Q.; Walker, Philip A.;

Vorlaender, Matthias K.; Bianchi, S.; Guarino, B.; De Marco, A.; Vanzetta, F.; Agatic, G.; Foglierini, M.; Pinna, D.; Fernandez-Rodriguez, B.; Fruehwirth, A.; Silacci, C.; Ogrodowicz, Roksana W.; Martin, Stephen R.; Sallusto, F.; Suzich, JoAnn A.; Lanzavecchia, A.; Zhu, Q.; Gamblin, Steven J.; Skehel, John J. Structure and Function Analysis of an Antibody Recognizing All Influenza A Subtypes. *Cell* **2016**, *166*, 596-608.

(16) Norde, W.; Lyklema, J. The Adsorption of Human Plasma Albumin and Bovine Pancreas Ribonuclease at Negatively Charged Polystyrene Surfaces. *Journal of Colloid and Interface Science* **1978**, *66*, 285-294.

(17) Cuypers, P.; Hermens, W. T.; Hemker, H. Ellipsometry as a Tool to Study Protein Films at Liquid-Solid Interfaces. *Analytical Biochemistry* **1978**, *84*, 56-67.

(18) Geoghegan, W. D.; Ackerman, G. A. Adsorption of Horseradish Peroxidase, Ovomuroid and Anti-Immunoglobulin to Colloidal Gold for the Indirect Detection of Concanavalin A, Wheat Germ Agglutinin and Goat Anti-Human Immunoglobulin G on Cell Surfaces at the Electron Microscopic Level: A New Method, Theory and Application. *Journal of Histochemistry & Cytochemistry* **1977**, *25*, 1187-1200.

(19) Lin, P.-C.; Chen, S.-H.; Wang, K.-Y.; Chen, M.-L.; Adak, A. K.; Hwu, J.-R. R.; Chen, Y.-J.; Lin, C.-C. Fabrication of Oriented Antibody-Conjugated Magnetic Nanoprobes and Their Immunoaffinity Application. *Analytical Chemistry* **2009**, *81*, 8774-8782.

(20) Wagner, P.; Hegner, M.; Kernen, P.; Zaugg, F.; Semenza, G. Covalent Immobilization of Native Biomolecules onto Au (111) Via N-Hydroxysuccinimide Ester Functionalized Self-Assembled Monolayers for Scanning Probe Microscopy. *Biophysical Journal* **1996**, *70*, 2052.

(21) Lim, C. Y.; Owens, N. A.; Wampler, R. D.; Ying, Y.; Granger, J. H.; Porter, M. D.; Takahashi, M.; Shimazu, K. Succinimidyl Ester Surface Chemistry: Implications of the



Competition between Aminolysis and Hydrolysis on Covalent Protein Immobilization. *Langmuir* **2014**, *30*, 12868-12878.

(22) Bae, Y. M.; Oh, B.-K.; Lee, W.; Lee, W. H.; Choi, J.-W. Study on Orientation of Immunoglobulin G on Protein G Layer. *Biosensors and Bioelectronics* **2005**, *21*, 103-110.

(23) Haugland, R. P. *Handbook of Fluorescent Probes and Research Products*; Molecular Probes, 2002.

(24) Verkleij, A. J.; Leunissen, J. L. *Immuno-Gold-Labeling in Cell Biology*; CRC Press, 1989.

(25) Turkevich, J.; Stevenson, P. C.; Hillier, J. A Study of the Nucleation and Growth Processes in the Synthesis of Colloidal Gold. *Discussions of the Faraday Society* **1951**, *11*, 55-75.

(26) Wikipedia. Dynamic Light Scattering: File: DLS.svg.

<https://en.wikipedia.org/wiki/File:DLS.svg> (accessed March 20, 2017).

(27) Zheng, T.; Bott, S.; Huo, Q. Techniques for Accurate Sizing of Gold Nanoparticles Using Dynamic Light Scattering with Particular Application to Chemical and Biological Sensing Based on Aggregate Formation. *ACS Applied Materials & Interfaces* **2016**, *8*, 21585-21594.

(28) Carr, B.; Wright, M. Nanoparticle Tracking Analysis. *Innovations in Pharmaceutical Technology* **2008**, *26*, 38-40.

(29) Walkey, C. D.; Olsen, J. B.; Guo, H.; Emili, A.; Chan, W. C. W. Nanoparticle Size and Surface Chemistry Determine Serum Protein Adsorption and Macrophage Uptake. *Journal of the American Chemical Society* **2012**, *134*, 2139-2147.

(30) Vertegel, A. A.; Siegel, R. W.; Dordick, J. S. Silica Nanoparticle Size Influences the Structure and Enzymatic Activity of Adsorbed Lysozyme. *Langmuir* **2004**, *20*, 6800-6807.

(31) Pollitt, M. J.; Buckton, G.; Piper, R.; Brocchini, S. Measuring Antibody Coatings on Gold Nanoparticles by Optical Spectroscopy. *RSC Advances* **2015**, *5*, 24521-24527.

- (32) Bell, N. C.; Minelli, C.; Shard, A. G. Quantitation of Igg Protein Adsorption to Gold Nanoparticles Using Particle Size Measurement. *Analytical Methods* **2013**, *5*, 4591-4601.
- (33) Khlebtsov, N. G.; Bogatyrev, V. A.; Dykman, L. A.; Melnikov, A. G. Spectral Extinction of Colloidal Gold and Its Biospecific Conjugates. *Journal of Colloid and Interface Science* **1996**, *180*, 436-445.
- (34) Minelli, C.; Garcia-Diez, R.; Sikora, A. E.; Gollwitzer, C.; Krumrey, M.; Shard, A. G. Characterization of Igg-Protein-Coated Polymeric Nanoparticles Using Complementary Particle Sizing Techniques. *Surface and Interface Analysis* **2014**, *46*, 663-667.
- (35) Monopoli, M. P.; Walczyk, D.; Campbell, A.; Elia, G.; Lynch, I.; Baldelli Bombelli, F.; Dawson, K. A. Physical–Chemical Aspects of Protein Corona: Relevance to in Vitro and in Vivo Biological Impacts of Nanoparticles. *Journal of the American Chemical Society* **2011**, *133*, 2525-2534.
- (36) Filbrun, S. L.; Driskell, J. D. A Fluorescence-Based Method to Directly Quantify Antibodies Immobilized on Gold Nanoparticles. *Analyst* **2016**, *141*, 3851-3857.
- (37) Jans, H.; Huo, Q. Gold Nanoparticle-Enabled Biological and Chemical Detection and Analysis. *Chemical Society Reviews* **2012**, *41*, 2849-2866.
- (38) Li, Y.; Schluesener, H. J.; Xu, S. Gold Nanoparticle-Based Biosensors. *Gold Bulletin* **2010**, *43*, 29-41.
- (39) Saha, K.; Agasti, S. S.; Kim, C.; Li, X.; Rotello, V. M. Gold Nanoparticles in Chemical and Biological Sensing. *Chemical Reviews* **2012**, *112*, 2739-2779.
- (40) Zeng, S.; Yong, K.-T.; Roy, I.; Dinh, X.-Q.; Yu, X.; Luan, F. A Review on Functionalized Gold Nanoparticles for Biosensing Applications. *Plasmonics* **2011**, *6*, 491-506.

- (41) Baniukevic, J.; Hakki Boyaci, I.; Goktug Bozkurt, A.; Tamer, U.; Ramanavicius, A.; Ramanaviciene, A. Magnetic Gold Nanoparticles in Sers-Based Sandwich Immunoassay for Antigen Detection by Well Oriented Antibodies. *Biosensors and Bioelectronics* **2013**, *43*, 281-288.
- (42) Parolo, C.; de la Escosura-Muñiz, A.; Polo, E.; Grazú, V.; de la Fuente, J. M.; Merkoçi, A. Design, Preparation, and Evaluation of a Fixed-Orientation Antibody/Gold-Nanoparticle Conjugate as an Immunosensing Label. *ACS Applied Materials & Interfaces* **2013**, *5*, 10753-10759.
- (43) Worsley, G. J.; Kumarswami, N.; Minelli, C.; Noble, J. E. Characterisation of Antibody Conjugated Particles and Their Influence on Diagnostic Assay Response. *Analytical Methods* **2015**, *7*, 9596-9603.
- (44) Walkey, C. D.; Olsen, J. B.; Guo, H.; Emili, A.; Chan, W. C. W. Nanoparticle Size and Surface Chemistry Determine Serum Protein Adsorption and Macrophage Uptake. *Journal of the American Chemical Society* **2012**, *134*, 2139-2147.
- (45) Horbett, T. A.; Cheng, C. M.; Ratner, B. D.; Hoffman, A. S.; Hanson, S. R. The Kinetics of Baboon Fibrinogen Adsorption to Polymers: In Vitro and in Vivo Studies. *Journal of Biomedical Materials Research* **1986**, *20*, 739-772.
- (46) Lopez, A.; Lovato, F.; Hwan Oh, S.; Lai, Y. H.; Filbrun, S.; Driskell, E. A.; Driskell, J. D. Sers Immunoassay Based on the Capture and Concentration of Antigen-Assembled Gold Nanoparticles. *Talanta* **2016**, *146*, 388-393.
- (47) Bell, N. C.; Minelli, C.; Shard, A. G. Quantitation of Igg Protein Adsorption to Gold Nanoparticles Using Particle Size Measurement. *Analytical Methods* **2013**, *5*, 4591-4601.

- (48) Khlebtsov, N. G.; Bogatyrev, V. A.; Dykman, L. A.; Melnikov, A. G. Spectral Extinction of Colloidal Gold and Its Biospecific Conjugates. *Journal of Colloid and Interface Science* **1996**, *180*, 436-445.
- (49) Pollitt, M. J.; Buckton, G.; Piper, R.; Brocchini, S. Measuring Antibody Coatings on Gold Nanoparticles by Optical Spectroscopy. *RSC Advances* **2015**, *5*, 24521-24527.
- (50) Minelli, C.; Garcia-Diez, R.; Sikora, A. E.; Gollwitzer, C.; Krumrey, M.; Shard, A. G. Characterization of IgG-Protein-Coated Polymeric Nanoparticles Using Complementary Particle Sizing Techniques. *Surface and Interface Analysis* **2014**, *46*, 663-667.
- (51) Monopoli, M. P.; Walczyk, D.; Campbell, A.; Elia, G.; Lynch, I.; Baldelli Bombelli, F.; Dawson, K. A. Physical–Chemical Aspects of Protein Corona: Relevance to in Vitro and in Vivo Biological Impacts of Nanoparticles. *Journal of the American Chemical Society* **2011**, *133*, 2525-2534.
- (52) Brewer, S. H.; Glomm, W. R.; Johnson, M. C.; Knag, M. K.; Franzen, S. Probing Bsa Binding to Citrate-Coated Gold Nanoparticles and Surfaces. *Langmuir* **2005**, *21*, 9303-9307.
- (53) Casals, E.; Pfaller, T.; Duschl, A.; Oostingh, G. J.; Puntès, V. Time Evolution of the Nanoparticle Protein Corona. *ACS Nano* **2010**, *4*, 3623-3632.
- (54) Lees, E. E.; Gunzburg, M. J.; Nguyen, T.-L.; Howlett, G. J.; Rothacker, J.; Nice, E. C.; Clayton, A. H. A.; Mulvaney, P. Experimental Determination of Quantum Dot Size Distributions, Ligand Packing Densities, and Bioconjugation Using Analytical Ultracentrifugation. *Nano Letters* **2008**, *8*, 2883-2890.
- (55) Guha, S.; Ma, X.; Tarlov, M. J.; Zachariah, M. R. Quantifying Ligand Adsorption to Nanoparticles Using Tandem Differential Mobility Mass Analysis. *Analytical Chemistry* **2012**, *84*, 6308-6311.

- (56) Jones, L. J.; Haugland, R. P.; Singer, V. L. Development and Characterization of the Nanorange Protein Quantitation Assay: A Fluorescence-Based Assay of Proteins in Solution. *BioTechniques* **2003**, *34*, 850-861.
- (57) Roach, P.; Shirtcliffe, N. J.; Farrar, D.; Perry, C. C. Quantification of Surface-Bound Proteins by Fluorometric Assay: Comparison with Quartz Crystal Microbalance and Amido Black Assay. *The Journal of Physical Chemistry B* **2006**, *110*, 20572-20579.
- (58) Geoghegan, W. D. The Effect of Three Variables on Adsorption of Rabbit IgG to Colloidal Gold. *Journal of Histochemistry & Cytochemistry* **1988**, *36*, 401-407.
- (59) Geoghegan, W. D.; Ackerman, G. A. Adsorption of Horseradish-Peroxidase, Ovomuroid and Antiimmunoglobulin to Colloidal Gold for Indirect Detection of Concanavalin-a, Wheat-Germ Agglutinin and Goat Antihuman Immunoglobulin-G on Cell-Surfaces at Electron-Microscopic Level - New Method, Theory and Application. *Journal of Histochemistry & Cytochemistry* **1977**, *25*, 1187-1200.
- (60) Horisberger, M. In *Immuno-Gold Labeling in Cell Biology*, Verkleij, A. J.; Leunissen, J. L. M., Eds.; CRC Press, Inc.: Boca Raton, FL, 1989, pp 50-60.
- (61) Xu, H.; Lu, J. R.; Williams, D. E. Effect of Surface Packing Density of Interfacially Adsorbed Monoclonal Antibody on the Binding of Hormonal Antigen Human Chorionic Gonadotrophin. *The Journal of Physical Chemistry B* **2006**, *110*, 1907-1914.
- (62) Zhou, C.; Friedt, J.-M.; Angelova, A.; Choi, K.-H.; Laureyn, W.; Frederix, F.; Francis, L. A.; Campitelli, A.; Engelborghs, Y.; Borghs, G. Human Immunoglobulin Adsorption Investigated by Means of Quartz Crystal Microbalance Dissipation, Atomic Force Microscopy, Surface Acoustic Wave, and Surface Plasmon Resonance Techniques. *Langmuir* **2004**, *20*, 5870-5878.

- (63) Dominguez-Medina, S.; McDonough, S.; Swanglap, P.; Landes, C. F.; Link, S. In Situ Measurement of Bovine Serum Albumin Interaction with Gold Nanospheres. *Langmuir* **2012**, *28*, 9131-9139.
- (64) Rocker, C.; Potzl, M.; Zhang, F.; Parak, W. J.; Nienhaus, G. U. A Quantitative Fluorescence Study of Protein Monolayer Formation on Colloidal Nanoparticles. *Nature Nanotechnology* **2009**, *4*, 577-580.
- (65) Meissner, J.; Prause, A.; Bharti, B.; Findenegg, G. H. Characterization of Protein Adsorption onto Silica Nanoparticles: Influence of Ph and Ionic Strength. *Colloid and Polymer Science* **2015**, *293*, 3381-3391.
- (66) Green, T. A. Gold Etching for Microfabrication. *Gold Bulletin* **2014**, *47*, 205-216.
- (67) Penn, M. A.; Drake, D. M.; Driskell, J. D. Accelerated Surface-Enhanced Raman Spectroscopy (Sers)-Based Immunoassay on a Gold-Plated Membrane. *Analytical Chemistry* **2013**, *85*, 8609-8617.
- (68) Wang, G. F.; Park, H. Y.; Lipert, R. J. Mixed Monolayers on Gold Nanoparticle Labels for Multiplexed Surface-Enhanced Raman Scattering Based Immunoassays. *Analytical Chemistry* **2009**, *81*, 9643-9650.
- (69) Saha, K.; Agasti, S. S.; Kim, C.; Li, X.; Rotello, V. M. Gold Nanoparticles in Chemical and Biological Sensing. *Chemical Reviews* **2012**, *112*, 2739-2779.
- (70) Reichert, J. M.; Valge-Archer, V. E. Development Trends for Monoclonal Antibody Cancer Therapeutics. *Nature Reviews Drug Discovery* **2007**, *6*, 349-356.
- (71) Conroy, P. J.; Hearty, S.; Leonard, P.; O'Kennedy, R. J. Antibody Production, Design and Use for Biosensor-Based Applications. *Seminars in Cell & Developmental Biology* **2009**, *20*, 10-26.

- (72) Smith, E.; Jager, B. The Characterization of Antibodies. *Annual Reviews in Microbiology* **1952**, *6*, 207-228.
- (73) Lynch, I.; Dawson, K. A. Protein-Nanoparticle Interactions. *Nano Today* **2008**, *3*, 40-47.
- (74) Puertas, S.; Batalla, P.; Moros, M.; Polo, E.; del Pino, P.; Guisán, J. M.; Grazú, V.; de la Fuente, J. M. Taking Advantage of Unspecific Interactions to Produce Highly Active Magnetic Nanoparticle–Antibody Conjugates. *ACS Nano* **2011**, *5*, 4521-4528.
- (75) Puertas, S.; de Gracia Villa, M.; Mendoza, E.; Jiménez-Jorquera, C.; de la Fuente, J. M.; Fernández-Sánchez, C.; Grazú, V. Improving Immunosensor Performance through Oriented Immobilization of Antibodies on Carbon Nanotube Composite Surfaces. *Biosensors and Bioelectronics* **2013**, *43*, 274-280.
- (76) van der Heide, S.; Russell, D. A. Optimisation of Immuno-Gold Nanoparticle Complexes for Antigen Detection. *Journal of Colloid and Interface Science* **2016**, *471*, 127-135.
- (77) Mustafaoglu, N.; Alves, N. J.; Bilgicer, B. Oriented Immobilization of Fab Fragments by Site-Specific Biotinylation at the Conserved Nucleotide Binding Site for Enhanced Antigen Detection. *Langmuir* **2015**, *31*, 9728-9736.
- (78) Mandl, A.; Filbrun, S. L.; Driskell, J. D. Asymmetrically Functionalized Antibody–Gold Nanoparticle Conjugates to Form Stable Antigen-Assembled Dimers. *Bioconjugate Chemistry* **2016**.
- (79) Kumar, S.; Aaron, J.; Sokolov, K. Directional Conjugation of Antibodies to Nanoparticles for Synthesis of Multiplexed Optical Contrast Agents with Both Delivery and Targeting Moieties. *Nature Protocols* **2008**, *3*, 314-320.
- (80) Yan, Q.; Zheng, H.-N.; Jiang, C.; Li, K.; Xiao, S.-J. Edc/Nhs Activation Mechanism of Polymethacrylic Acid: Anhydride Versus Nhs-Ester. *RSC Advances* **2015**, *5*, 69939-69947.

- (81) Montenegro, J.-M.; Grazu, V.; Sukhanova, A.; Agarwal, S.; Jesus, M.; Nabiev, I.; Greiner, A.; Parak, W. J. Controlled Antibody/(Bio-) Conjugation of Inorganic Nanoparticles for Targeted Delivery. *Advanced Drug Delivery Reviews* **2013**, *65*, 677-688.
- (82) Raghav, R.; Srivastava, S. Immobilization Strategy for Enhancing Sensitivity of Immunosensors: L-Asparagine–AuNPs as a Promising Alternative of EDC–NHS Activated Citrate–AuNPs for Antibody Immobilization. *Biosensors and Bioelectronics* **2016**, *78*, 396-403.
- (83) Jazayeri, M. H.; Amani, H.; Pourfatollah, A. A.; Pazoki-Toroudi, H.; Moghadam, B. S. Various Methods of Gold Nanoparticles (GNPs) Conjugation to Antibodies. *Sensing and Bio-Sensing Research* **2016**.
- (84) Duval, F.; van Beek, T. A.; Zuilhof, H. Key Steps Towards the Oriented Immobilization of Antibodies Using Boronic Acids. *Analyst* **2015**, *140*, 6467-6472.
- (85) Wagner, P.; Hegner, M.; Kernen, P.; Zaugg, F.; Semenza, G. Covalent Immobilization of Native Biomolecules onto Au (111) Via N-Hydroxysuccinimide Ester Functionalized Self-Assembled Monolayers for Scanning Probe Microscopy. *Biophysical Journal* **1996**, *70*, 2052-2066.
- (86) Pei, Z.; Anderson, H.; Myrskog, A.; Dunér, G.; Ingemarsson, B.; Aastrup, T. Optimizing Immobilization on Two-Dimensional Carboxyl Surface: pH Dependence of Antibody Orientation and Antigen Binding Capacity. *Analytical Biochemistry* **2010**, *398*, 161-168.
- (87) Mu, B.; Huang, X.; Bu, P.; Zhuang, J.; Cheng, Z.; Feng, J.; Yang, D.; Dong, C.; Zhang, J.; Yan, X. Influenza Virus Detection with Pentabody-Activated Nanoparticles. *Journal of Virological Methods* **2010**, *169*, 282-289.



- (88) Xu, Q.; Xu, H.; Gu, H.; Li, J.; Wang, Y.; Wei, M. Development of Lateral Flow Immunoassay System Based on Superparamagnetic Nanobeads as Labels for Rapid Quantitative Detection of Cardiac Troponin I. *Materials Science and Engineering: C* **2009**, *29*, 702-707.
- (89) Yang, J.; Lee, C.-H.; Park, J.; Seo, S.; Lim, E.-K.; Song, Y. J.; Suh, J.-S.; Yoon, H.-G.; Huh, Y.-M.; Haam, S. Antibody Conjugated Magnetic P1ga Nanoparticles for Diagnosis and Treatment of Breast Cancer. *Journal of Materials Chemistry* **2007**, *17*, 2695-2699.
- (90) Jiang, K.; Schadler, L. S.; Siegel, R. W.; Zhang, X.; Zhang, H.; Terrones, M. Protein Immobilization on Carbon Nanotubes Via a Two-Step Process of Diimide-Activated Amidation. *Journal of Materials Chemistry* **2004**, *14*, 37-39.
- (91) Patel, N.; Davies, M. C.; Hartshorne, M.; Heaton, R. J.; Roberts, C. J.; Tendler, S. J.; Williams, P. M. Immobilization of Protein Molecules onto Homogeneous and Mixed Carboxylate-Terminated Self-Assembled Monolayers. *Langmuir* **1997**, *13*, 6485-6490.
- (92) Rohde, R. D.; Agnew, H. D.; Yeo, W.-S.; Bailey, R. C.; Heath, J. R. A Non-Oxidative Approach toward Chemically and Electrochemically Functionalizing Si (111). *Journal of the American Chemical Society* **2006**, *128*, 9518-9525.
- (93) Frey, B. L.; Corn, R. M. Covalent Attachment and Derivatization of Poly (L-Lysine) Monolayers on Gold Surfaces as Characterized by Polarization- Modulation Ft-Ir Spectroscopy. *Analytical Chemistry* **1996**, *68*, 3187-3193.
- (94) Guler, Z.; Sarac, A. Electrochemical Impedance and Spectroscopy Study of the EDC/NHS Activation of the Carboxyl Groups on Poly (E-Caprolactone)/Poly (M-Anthranilic Acid) Nanofibers. *Express Polymer Letters* **2016**, *10*.
- (95) Chiodi, F.; Sidén, Å.; Ösby, E. Isoelectric Focusing of Monoclonal Immunoglobulin G, a and M Followed by Detection with the Avidin-Biotin System. *Electrophoresis* **1985**, *6*, 124-128.